

# Non-perturbative materialization of ghosts

Roberto Emparan<sup>a,b</sup> and Jaume Garriga<sup>a</sup>

<sup>a</sup>*Departament de Física Fonamental*

*Universitat de Barcelona, Diagonal 647, E-08028, Barcelona, Spain*

<sup>b</sup>*Institució Catalana de Recerca i Estudis Avançats (ICREA)*

emparan@ub.edu, garriga@ifae.es

## Abstract

In theories with a hidden ghost sector that couples to visible matter through gravity only, empty space can decay into ghosts and ordinary matter by graviton exchange. Perturbatively, such processes can be very slow provided that the gravity sector violates Lorentz invariance above some cut-off scale. Here, we investigate non-perturbative decay processes involving ghosts, such as the spontaneous creation of self-gravitating lumps of ghost matter, as well as pairs of Bondi dipoles (*i.e.*, lumps of ghost matter chasing after positive energy objects). We find the corresponding instantons and calculate their Euclidean action. In some cases, the instantons induce topology change or have negative Euclidean action. To shed some light on the meaning of such peculiarities, we also consider the nucleation of concentric domain walls of ordinary and ghost matter, where the Euclidean calculation can be compared with the canonical (Lorentzian) description of tunneling. We conclude that non-perturbative ghost nucleation processes can be safely suppressed in phenomenological scenarios.

# 1 Introduction

Recently it has been suggested that the smallness of the observed cosmological constant can be attributed to an approximate “energy symmetry” [1]. The idea is that Nature is endowed with an exact copy of the matter sector, but with an overall minus sign in the action [2, 1],

$$\mathcal{L} = \sqrt{-g}\{M_P^2 R + \mathcal{L}_{\text{matt}}(\psi, g) - \mathcal{L}_{\text{matt}}(\hat{\psi}, g) + \dots\}. \quad (1)$$

Here,  $g$  is the metric,  $\psi$  are ordinary matter fields (including those of the Standard Model), and  $\hat{\psi}$  are the ghost fields. Energy parity is defined by  $\psi \rightarrow \hat{\psi}$ ,  $\hat{\psi} \rightarrow \psi$ ,  $g \rightarrow g$ . Ignoring gravity, the Hamiltonian  $H$  transforms as

$$H \rightarrow -H. \quad (2)$$

The vacuum state  $|0\rangle$  is defined as parity invariant, and from (2) the corresponding vacuum energy vanishes to all orders in perturbation theory. However, gravity breaks the energy symmetry and a cosmological constant is induced. It was argued in [1] that the magnitude of this vacuum energy can be comparable to the one suggested by observations provided that the gravitational cut-off scale  $\mu$  is sufficiently low (lower than the inverse of 30 microns, about an order of magnitude beyond the reaches of ongoing short distance probes of gravity).

“Phantom” matter has also been invoked in phenomenological studies of dark energy [3, 4, 5], as a way of obtaining an effective equation of state parameter  $w < -1$ . This violates all the standard energy conditions, but is not at all disfavoured by observations. A ghost sector is also present in the recently proposed B-inflation, based on effective theories with only second derivatives of a scalar field [6].

In all of these cases, the Hamiltonian is unbounded below, and disaster would follow unless one postulates that the Lorentz symmetry is broken at a certain energy scale [5]. The reason is simple. In the model (1), empty space can decay into a pair of  $\psi$  ordinary particles and a pair of  $\hat{\psi}$  ghost particles

$$|0\rangle \rightarrow \psi\psi\hat{\psi}\hat{\psi} \quad (3)$$

(if particles are charged, one in each pair should be understood as the antiparticle). Let the momenta of the ordinary particles be  $p_1$  and  $p_2$ , and the momenta of the ghost particles  $k_1$  and  $k_2$ . From translation invariance, the decay amplitude takes the form  $\langle p_1, p_2, k_1, k_2 | 0 \rangle = \mathcal{A}(p_1, p_2, k_1, k_2) \delta^{(4)}(p_1 + p_2 + k_1 + k_2)$ , which after integration over external momenta leads to the vacuum decay rate per unit volume

$$\Gamma = \int d^4P \gamma(P), \quad (4)$$

where  $\gamma(P) = \int d\tilde{p}_1 d\tilde{p}_2 d\tilde{k}_1 d\tilde{k}_2 |\mathcal{A}|^2 \delta^{(4)}(P+k_1+k_2) \delta^{(4)}(P-p_1-p_2)$ . In a Lorentz invariant theory,  $\gamma(P)$  is just a function of  $s = -P_\mu P^\mu$ , and Defining  $\vec{v} = s^{-1/2} \vec{P}$ , we have

$$\Gamma = \int ds s \gamma(s) \int \frac{d^3 \vec{v}}{2\sqrt{1+v^2}}. \quad (5)$$

Physically, the last integral corresponds to the fact that there is no preferred reference frame, and the total momentum  $P^\mu$  of the pair of particles (or the pair of ghosts) is equally likely to fall anywhere on the mass-shell of radius  $s^{1/2}$ . Particles only interact with ghosts gravitationally, and so the momentum  $P^\mu$  is transferred by gravitons. The decay rate is in principle infinite (due to the mass-shell integral) but it can be rendered finite if we postulate that Lorentz invariance is broken in the gravitational sector at some scale  $\mathcal{E}$  [5]. The remaining integral over  $s$  can be finite in a theory where gravity becomes soft at a certain cut-off scale  $\mu$ , as it is in fact assumed. The process becomes completely negligible if  $\mathcal{E}$  is comparable to the cut-off scale  $\mu \lesssim (30 \mu\text{m})^{-1}$  discussed above [1]. Similarly, empty space can decay to ghosts  $\hat{\psi}$  and gravitons  $h$ ,<sup>1</sup>

$$|0\rangle \rightarrow hh\hat{\psi}\hat{\psi}. \quad (6)$$

In this case, the integrals over the momenta of the external gravitons must be cut-off at the Lorentz violating energy scale  $\mathcal{E}$ . In this way, the vacuum can be made sufficiently stable to perturbative decay processes, in spite of the ghosts [1, 4].

Although perturbative processes may be suppressed by the Lorentz-violating physics, it is conceivable that non-perturbative processes may quickly destabilize the present vacuum, through the production of lumps of non-relativistic ghost matter. The purpose of the present paper is to investigate the non-perturbative analogues of (3) and (6). Decays that proceed via non-perturbative tunneling are typically slower than their perturbative counterparts, but when ghosts are involved there are several reasons why this is not so obvious.

In accordance with the equivalence principle, a lump of ghost matter tends to fall towards the potential well created by a positive energy object. On the other hand, the repulsive gravitational field it produces tends to push the positive energy object away. It has been known for some time that this leads to a runaway behaviour, where the positive energy object is chased after by the ghost [7, 8, 9, 10], with a constant acceleration. Such configuration is known as a *Bondi dipole* [7]. As we shall see, such self-accelerating solutions can be continued to the Euclidean section, leading to a semiclassical description of the spontaneous nucleation of pairs of Bondi dipoles. This would be the non-perturbative analogue of (3). A simple estimate (which we will confirm by rigorous calculation) gives the Euclidean action

---

<sup>1</sup>Ref. [1] actually considered the decay  $|0\rangle \rightarrow h^*\hat{\psi}\hat{\psi}$ , where  $h^*$  is an “excited” (soft-scale) graviton, which is a more dominant process than (6). We shall not consider the non-perturbative analogue of this process, since it cannot be described in terms of the low energy effective action (1).

of this process as  $\sim m_+ d$ , where  $d$  is the size of the dipole and  $m_+$  is the mass of its ordinary positive-mass component. Even if we impose  $d \gtrsim \mu^{-1}$ , we see that the action can dangerously approach a value of order one if the Compton wavelength of the particles produced is also close to the gravitational cutoff.

The analogue of (6) is the pair creation of self-gravitating lumps of ghost matter, which repel each other. The possibility of this process is suggested by the following weak field argument. The interaction energy of two ghost particles at rest, with identical mass  $m < 0$ , is given by  $E_{grav} = Gm^2/2r$ . Here  $G$  is Newton's constant and  $2r$  is the distance between the masses. For  $r = -Gm/4$  the positive gravitational energy is equal to minus the rest mass energy of the pair  $E_{grav} = -2m$ , so this configuration can in principle pop out of the vacuum without violating energy conservation. Also, the initial acceleration of each particle is given by  $a = 1/r$ , suggesting that there is a Euclidean solution where the ghost matter runs around a circle of radius  $1/a$ . Note, however, that for  $r \sim -Gm$  the gravitational field is of order one, and non-linear gravity must be taken into account. The corresponding instantons still exist, and have interesting peculiarities which make their interpretation non-trivial. First of all, they can produce a topology change, and second, the corresponding Euclidean action (defined as the bounce action minus the background action) can be *negative*.

To shed some light into the meaning of such peculiarities, we shall first consider the simpler example of vacuum decay in a theory where the matter and the ghost sectors support domain wall solutions. In this case, the process of spontaneous nucleation of concentric spherical domain walls of ordinary and ghost matter chasing after each other is the analogue of (3). The analogue of (6) is the spontaneous creation of spherical domain walls of ghost matter. If the cosmological constant is exactly vanishing, the instanton for the latter process changes the topology of space and a new boundary appears inside of the domain wall. This makes the calculation of the corresponding Euclidean action somewhat ill-defined. On the other hand, in the presence of a small cosmological constant (such as the one present in our universe), the topology does not change at all and the Euclidean action can be calculated unambiguously. Interestingly, it turns out to be negative. These features are quite similar to what happens in the case of pair creation of lumps of ghost matter, but the advantage here is that the geometry is much simpler, and the Euclidean calculation can be compared with a canonical (Lorentzian) description of tunneling.

The plan of the paper is the following. Since the subject of tunneling in theories with ghosts is fraught with many subtleties, we have developed it in quite some detail in Sections 2 through 4. The specific application of our results to the energy-symmetric scenario of [1] is then discussed in the concluding Section 5, to which phenomenologically-minded readers might want to jump directly if not interested in the theory of ghost tunneling.

The more technical sections 2–4 consist of a discussion of: the spontaneous nucleation of domain walls (Section 2); the pair creation of Bondi dipoles, *i.e.*, the non-perturbative analogue of (3) (Section 3, where also we briefly review several technical aspects of the axisymmetric class of solutions for the benefit of readers unfamiliar with them); the spontaneous creation of self-gravitating lumps of ghost matter, *i.e.*, the non-perturbative analogue of (6) (Section 4). Some details of the canonical WKB construction of tunneling paths are deferred to an Appendix.

## 2 Ghosts through the tunnel

In field theory, semiclassical tunneling rates are usually estimated through the expression

$$\Gamma \sim e^{-I_E}. \quad (7)$$

Here,  $I_E$  is the action of the Euclidean instanton describing the decay, minus the action of the background, and we have omitted the prefactor arising from integration of fluctuations around these solutions. For ordinary fields, with the rotation  $t = it_E$ , the Euclidean action is positive definite,  $I_E > 0$ , and the above formula gives an exponential suppression in the limit when the semiclassical approximation is valid,  $I_E \gg 1$ . With the same rotation  $t = it_E$ , the Euclidean action for ghost matter is negative definite,  $I_E < 0$ , and from a naive application of (7) one may be tempted to conclude that ghosts lead to catastrophic decay rates. However, this conclusion would be premature. Rather, the problem is that the Euclidean path integral is ill-defined: in order to make it convergent, ordinary matter and ghosts would require opposite Wick rotations. Hence, the standard Euclidean methods are not directly applicable in the present context.

For instance, in the limit when gravity is neglected  $G \rightarrow 0$ , the theory (1) is symmetric under energy parity. In this limit, ordinary and ghost matter are decoupled and have exactly the same dynamics. Note that, as a consequence, in *e.g.*, Schwinger pair production, it is just as hard to screen a ghost electric field by nucleation of charged ghosts, as it is to screen an ordinary electric field by nucleation of ordinary charged particles. So in both cases, instanton processes must be exponentially suppressed, as

$$\Gamma \sim e^{-|I_E|}. \quad (8)$$

Thus, when gravity is switched off, nonperturbative processes in the ghost sector will not bring any disaster, even if with the standard rotation the Euclidean action is negative.

When gravity is switched on, both sectors are coupled and, as mentioned above, the standard Euclidean methods do not apply. Hence, we should try to develop some understanding

of the problem from the canonical approach to tunneling. In the WKB approximation, the wave function is of the form  $\Psi \sim A \exp(iW) + B \exp(-iW)$ , where for a simple quantum mechanical system  $W(q) = \int^q p(q') dq'$ , and the integral is taken along a semiclassical trajectory. Under the barrier, the momentum  $p$  is imaginary and  $\Psi$  becomes a superposition of growing and decaying exponentials. We are interested in the situation where the wave function is outgoing after tunneling, so generically we have a comparable contribution of the growing and decaying modes at the turning point after the barrier. This means that the amplitude  $\Psi_a$  *after* the barrier is exponentially smaller than the amplitude  $\Psi_b$  *before* the barrier

$$|\Psi_a/\Psi_b|^2 \sim \exp(-2|\Delta W|) \quad (9)$$

Here,  $\Delta W$  is the difference in  $W$  evaluated at the two turning points. From this perspective, we should expect that a tunneling process is suppressed, whether it involves ghosts or not.

In order to gain some intuition on this problem, we shall consider in the following subsections the spontaneous nucleation of spherical domain walls. The dynamics of domain walls is sufficiently simple to be discussed in the canonical formalism. First, in Subsections 2.2, 2.3 and 2.4 we shall describe some instanton solutions which in the standard interpretation would correspond to the nucleation of walls in flat and in deSitter space. In Subsection 2.4 we consider the same processes in the canonical approach, without reference to Euclidean methods. Finally, in Subsection 2.5, and in the light of the examples considered, we elaborate on the possible relation between the Euclidean action and the nucleation rates.

## 2.1 Nucleation of diwalls from flat space

The gravitational field of an ordinary domain wall is repulsive [11]. On the other hand, a ghost wall will be attractive, and we may expect to find solutions where a wall of ghost matter is chased after by a wall of usual matter. By analogy with the Bondi dipoles discussed in the introduction, we may call such a configuration a *diwall*.

Domain walls are rather easy to treat as distributional sources in General Relativity. Their effect is a discontinuity in the extrinsic curvature  $K_{ab}$  accross the worldsheet [12]

$$[K_{ab}] = -4\pi G \sigma \gamma_{ab}, \quad (10)$$

where  $\sigma$  is the tension of the wall and  $\gamma_{ab}$  is the induced metric. Consider a Euclidean spherically symmetric solution with a wall of positive tension  $\sigma_1$  and a wall of negative tension  $-\sigma_2$ . The metric takes the form

$$ds^2 = dy^2 + R^2(y) d\Omega_3, \quad (11)$$

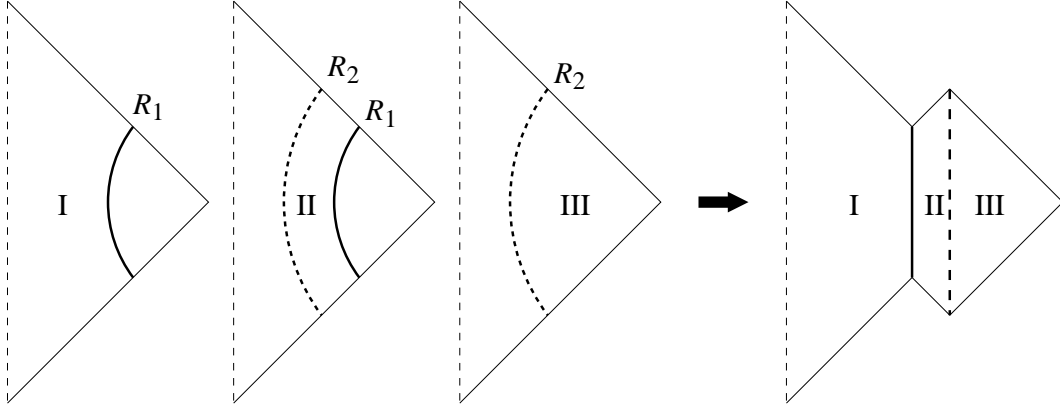


Figure 1: Conformal diagrams for the construction of the *diwall* solution. Three different regions (I, II, III) of Minkowski space are cut out at given radii  $R_1 > R_2$ , and pasted to form a wall of positive tension (thick solid line) at  $R_1$  and a ghost wall of negative tension (thick dashed line) at  $R_2$ . In the final diagram, moving towards the right corresponds to increasing radius in I and III, and to decreasing radius in II.

where  $d\Omega_3$  is the line element on the 3-sphere and  $y$  is a radial coordinate. Outside the sources, the metric is flat, and the warp factor  $R(y)$  is piecewise linear with slope  $dR/dy = \pm 1$ . At the location of the sources, the slope is discontinuous, to account for the jump in the extrinsic curvature. Hence, starting from the center of symmetry at  $y = 0$  the solution is given by (see fig. 1)

$$\begin{aligned}
 R(y) &= y & (0 < y < R_1), \\
 R(y) &= 2R_1 - y & (R_1 < y < 2R_1 - R_2), \\
 R(y) &= 2R_2 - 2R_1 + y & (2R_1 - R_2 < y < \infty).
 \end{aligned} \tag{12}$$

Eq. (10) demands that  $R_1 = 1/2\pi G\sigma_1$  and  $R_2 = 1/2\pi G\sigma_2$ . The radius  $R(y)$  of the 3-spheres increases up to  $R_1$ , backtracks to  $R_2$ , and then increases to infinity. Note that  $R_2 < R_1$ , which requires  $\sigma_2 > \sigma_1$ . For our illustrative purposes, we shall simply assume that the theory supports domain walls satisfying this inequality.

The solution Eq. (12) is perfectly regular and asymptotically flat. It can be thought of as a semiclassical trajectory which interpolates between flat empty space  $\mathbb{R}^3$  (at infinity), and the equatorial slice of the metric (11). This “turning point” slice contains two concentric domain walls of radii  $R_1$  and  $R_2$ .

After nucleation, the evolution is given by the analytic continuation of (11) to Lorentzian time, which converts the 3-spheres into time-like hyperboloids. In particular, the positive and negative tension walls expand with constant proper acceleration  $1/R_1$  and  $1/R_2$  respectively.

Due to the peculiar “backtracking” form of the metric between  $R_1$  and  $R_2$ , it is the wall of larger radius (and positive tension) which chases after the one of smaller radius (and negative tension) as they both expand. This is as it should be, since the wall of positive tension is repulsive and the other one is attractive.

The Euclidean action can be easily calculated from

$$I_E = -\frac{1}{16\pi G} \int d^4x \sqrt{g} \mathcal{R} + \sum_i s_i \sigma_i \int d^3\xi \sqrt{\gamma}, \quad (13)$$

where  $s_i$  is the sign of the wall tension (and  $\sigma_i$  is as usual its absolute value). On shell, the Ricci scalar is related to the source [13]

$$\sqrt{g} \mathcal{R} = 24\pi G \sigma \int d^3\xi \sqrt{\gamma} \delta^4(x - x(\xi)), \quad (14)$$

and integrating over the volume of the 3-spheres, we easily find

$$I_E^{diwall} = \frac{1}{8\pi G^3} (\sigma_2^{-2} - \sigma_1^{-2}) < 0. \quad (15)$$

Note that the Euclidean action is negative. In the limit  $\delta\sigma = \sigma_2 - \sigma_1 \ll \sigma$ , we have  $|I_E| \sim (M_P^6/\sigma^2)(\delta\sigma/\sigma)$ . This is likely to be very large, unless the wall tensions are very nearly degenerate, or unless they are very close to the Planck scale  $M_P$ .

The diwall instanton (12) is an analogue of the process (3), where ghost and ordinary matter are created from the vacuum. Let us now investigate the analogue of (6).

## 2.2 Ghost walls from flat space?

An instanton for a single spherical domain wall of negative tension in an asymptotically flat space can be constructed along the same lines as in the previous subsection. The warp factor is now given by (see fig. 2)

$$R(y) = |y| + R_2 \quad (-\infty < y < \infty). \quad (16)$$

From large radii ( $y \rightarrow \infty$ ), the worldsheet is seen as a spherical object of radius  $R_2$  embedded in an otherwise flat Euclidean space. However, if we cross the worldsheet towards negative  $y$ , we discover that the radius does not shrink to zero. Rather, it grows as we go in. This “throat” is of course an identical copy of the geometry for  $y > 0$ . The topology of the instanton is not  $\mathbb{R}^4$ , but  $\mathbb{R} \times S^3$ , and the solution has two disconnected boundaries, one at  $y \rightarrow \infty$  and another one “inside” the domain wall, at  $y \rightarrow -\infty$ .

Calculating the Euclidean action as we did in the previous subsection would yield

$$I_E = \frac{1}{\pi G^3 \sigma_2^2} > 0. \quad (17)$$



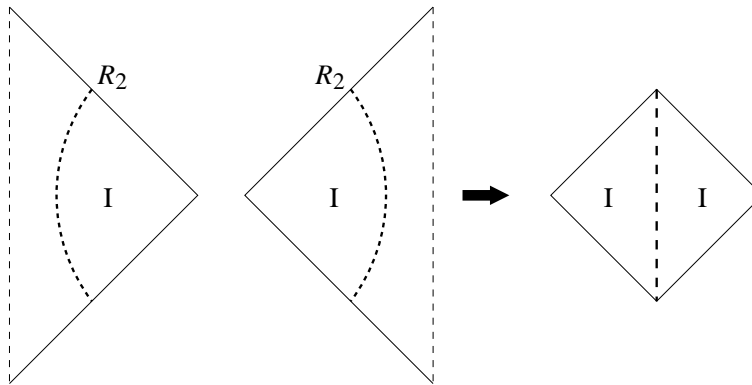


Figure 2: Construction of the ghost wall spacetime. Observe the presence of two disconnected asymptotic boundaries.

But the fact that the instanton has different topology than the background should give us pause. The Gibbons-Hawking boundary term  $I_E^b = -(8\pi G) \int d^3\xi \sqrt{\gamma} K$  at the new inner boundary ( $y \rightarrow -\infty$ ) is given by  $I_E^b = -3\pi R_c^2/4G < 0$ , where  $R_c$  is some large cut-off radius. It is unclear what subtraction (if any) should be performed on this divergent contribution, since the original flat space background does not include such inner boundary. Also, from a canonical point of view, it doesn't seem possible to go from the original  $\mathbb{R}^3$  to the final turning point geometry (with two asymptotically flat regions) by continuous slicing of the instanton. Because of that, the interpretation of the solution (16) as a semiclassical path describing the nucleation of a ghost wall remains unclear.

Fortunately, the situation is clarified by considering nucleation from a vacuum with a small cosmological constant.

### 2.3 Walls from deSitter space

As mentioned in the introduction, gravity breaks the energy symmetry (2). This may give rise the small observed cosmological constant  $\Lambda > 0$ . In this case, the Euclidean background is the 4-sphere of radius  $H^{-1} = (3/\Lambda)^{1/2}$ , with warp factor

$$R_b(y) = H^{-1} \sin(Hy), \quad (0 \leq Hy \leq \pi). \quad (18)$$

Nucleation of positive tension domain walls in deSitter has been thoroughly studied in Ref. [13]. The relevant instanton is constructed from two caps of the 4-sphere, joined at the worldsheet of the domain wall (which is an  $S^3$ ),

$$\begin{aligned} R_a(y) &= H^{-1} \sin(Hy), & (0 \leq Hy \leq \chi_0), \\ R_a(y) &= H^{-1} \sin(2\chi_0 - Hy), & (\chi_0 \leq Hy \leq 2\chi_0). \end{aligned} \quad (19)$$

The angular span  $\chi_0$  of the spherical cap is determined through the junction condition (10)

$$\tan \chi_0 = \frac{H}{2\pi G\sigma_1}, \quad (20)$$

where  $\sigma_1$  is the tension of the domain wall. Thus, the radius of the worldsheet is given by

$$R_w = R_a(y_0) = H^{-1} \sin \chi_0 = \frac{1}{\sqrt{H^2 + (2\pi G\sigma_1)^2}}. \quad (21)$$

The Euclidean action can be calculated from (13) with an additional vacuum energy term  $\frac{1}{8\pi G} \int d^4x \sqrt{g} \Lambda$ . On shell, we can use (14) as well as the bulk equations of motion  $\mathcal{R} = 4\Lambda$ .

Properly speaking, this instanton would describe the creation from nothing of a deSitter space containing a wall. If we want to describe instead the transition from empty deSitter to deSitter with a wall, then we must face the well-known problem that no non-singular instanton mediates between both spacetimes. For the time being, we will follow the common procedure of calculating the action for the whole process by subtracting the action  $I_{dS}$  of the background deSitter,

$$I_{dS} = -\frac{\pi}{GH^2}. \quad (22)$$

This will be justified in more detail in the next subsection. Some straightforward algebra leads to [13]

$$I_E^+ = \frac{2\pi^2\sigma_1}{H^2\sqrt{H^2 + (2\pi G\sigma_1)^2}} > 0. \quad (23)$$

Let us now consider the nucleation of negative tension walls in de Sitter. In fact, Eqs. (20-23) still hold, with the replacement  $\sigma_1 \rightarrow -\sigma_2$ . The angle  $\chi_0$ , determined by

$$\tan \chi_0 = -\frac{H}{2\pi G\sigma_2}, \quad (24)$$

will be larger than  $\pi/2$ , so instead of having two spherical caps glued to the worldsheet, it will now be two capped spheres which are glued. The corresponding euclidean action is negative

$$I_E^- = -\frac{2\pi^2\sigma_2}{H^2\sqrt{H^2 + (2\pi G\sigma_2)^2}} < 0. \quad (25)$$

Unlike the case of ghost walls from flat space discussed in the previous subsection, the topology of the instanton is here the same as for the deSitter background, and no additional boundaries appear. Note that in the limit of a small cosmological constant  $H \rightarrow 0$ , the action (25) tends to negative infinity, unlike the naive result (17).

In the limit of small tension, where the walls do not deform the geometry of deSitter, the equations of motion for positive and negative tension are exactly the same, and therefore it is expected on general grounds that it is just as hard to create a positive tension wall as it

is to create a negative tension one. Here, we find that  $|I_E|$  has the same form in both cases, which supports the use of Eq. (8) [rather than Eq. (7)] for the calculation of the nucleation rates.

It is interesting to observe also that  $|I_E|$  has the same form for both signs of the tension even when this tension is large and the background geometry is considerably deformed (note that the shape of the instantons for positive and negative tension walls is quite different in this case).

## 2.4 Canonical approach

In this subsection, we shall consider the processes discussed in the previous ones in the canonical WKB approach, without reference to Euclidean methods.

Let us consider the system of a spherically symmetric domain wall in the presence of a cosmological constant  $\Lambda \equiv 3H^2$ . Inside the wall, the metric is just empty deSitter space, whereas outside the wall, and by Birkhoff's theorem, the metric is Schwarzschild-deSitter, characterized by a mass parameter  $M$ . This system has a single degree of freedom, which is the radius of the wall. A domain wall of very small radius, and correspondingly very small mass  $M$ , can tunnel to a big domain wall of size comparable to the cosmological horizon (while the mass parameter  $M$  remains of course a small constant). In the limit when  $M \rightarrow 0$ , this process corresponds to the spontaneous nucleation of a large domain wall (from an infinitesimally small seed) in an otherwise empty deSitter space. This is schematically represented in Figs. 3 and 4 for the case of ordinary walls and ghost walls respectively.

In order to describe this process, we shall closely follow the procedure developed in Ref. [14]. The action is given by

$$I = \frac{1}{16\pi G} \int d^4x \sqrt{-g} \mathcal{R} - \frac{\Lambda}{8\pi G} \int d^4x \sqrt{-g} - \sigma \int d^3\xi \sqrt{-\gamma}. \quad (26)$$

The spherically symmetric metric takes the form

$$ds^2 = -(N^t)^2 dt^2 + L^2(dr + N^r dt)^2 + R^2 d\Omega_2, \quad (27)$$

where  $N^t, L$  and  $R$  are functions of  $r$  and  $t$ , and  $d\Omega_2$  is the metric on the two-sphere. The action can be written as

$$I = \int dt p \dot{q} + \int dr dt (\Pi_L \dot{L} + \Pi_R \dot{R} - N^t \mathcal{H}_t - N^r \mathcal{H}_r), \quad (28)$$

where  $q(t)$  is the radial coordinate  $r$  of the wall at time  $t$ , the momenta

$$\begin{aligned} p &= -4\pi\sigma R^2 L^2 (\dot{q} + N^r) [N^{t\ 2} - L^2 (\dot{q} + N^r)^2]^{-1/2}, \\ \Pi_R &= [(N^r L R)' - (L R)'] / G N^t, \\ \Pi_L &= R (N^r R' - \dot{R}) / G N^t. \end{aligned} \quad (29)$$

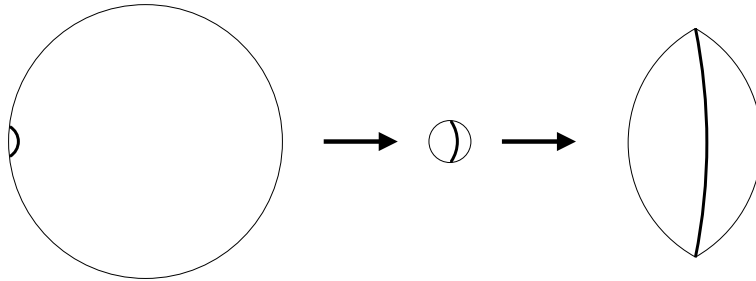


Figure 3: WKB path for the spontaneous nucleation of a domain wall of positive tension in deSitter. The leftmost figure represents the “initial” classical turning point 3-geometry before tunneling. It consists of a small domain wall of infinitesimal mass  $M$ . Inside the wall, the metric is a small cap of a 3-sphere of radius  $H^{-1}$  (which looks almost flat on the scale of the radius of the wall). Outside the wall, the geometry is a  $t = \text{constant}$  section of a Schwarzschild-deSitter metric with a very small mass. Classically, the small wall would shrink under its own tension and form a small black hole. However, it has a certain probability for tunneling into a big wall, of size comparable to the cosmological horizon, through a sequence of interpolating “underbarrier” 3-geometries (whose construction is described in Subsection 2.4 and in the Appendix). The “final” turning point geometry is represented in the rightmost figure. In the limit when  $M \rightarrow 0$ , this final turning point geometry consists of two large caps of a 3-sphere of radius  $H^{-1}$  glued at the wall. Note that the intermediate interpolating 3-geometries in such path shrink to a very small size, just a few times larger than the size of the initial domain wall. In the limit  $M \rightarrow 0$  this intermediate geometry would shrink to nothing. The initial and final geometries can also be thought of as equatorial slices of the deSitter instanton and of the domain wall instanton [given in Eq. (19)] respectively.

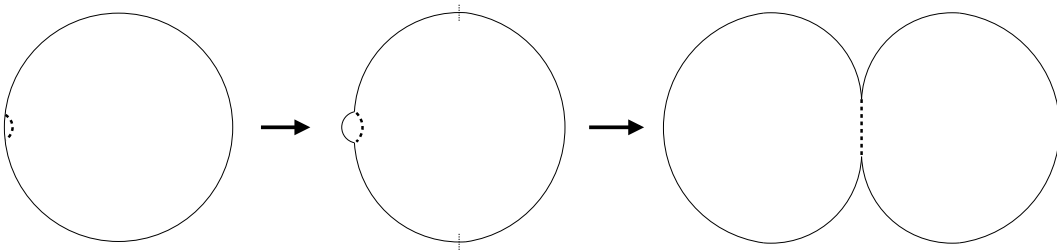


Figure 4: Same as Fig. 3 for a ghost domain wall. The final turning point geometry consists now of two capped 3-spheres of radius  $H^{-1}$ , which correspond to the equatorial slice of the instanton (19). As shown in the Appendix, another difference with the case of positive tension walls is that the volume of the intermediate three-geometry in the semiclassical path never shrinks to a very small size, even in the limit  $M \rightarrow 0$ .

are conjugate to  $q$ ,  $L$  and  $R$  respectively, and the Hamiltonian densities are given in terms of the canonical variables as

$$\mathcal{H}_t(r) = \frac{GL\Pi_L^2}{2R^2} - \frac{G\Pi_L\Pi_R}{R} + \frac{1}{2G} \left\{ \left( \frac{2RR'}{L} \right)' - \frac{R'^2}{L} - L \right\} + \frac{\Lambda LR^2}{2G} + \frac{E}{L} \delta(q-r), \quad (30)$$

$$\mathcal{H}_r(r) = R' \Pi_R - L \Pi_L' - p \delta(q-r). \quad (31)$$

Here  $E = \text{sign}(\sigma)(p^2 + 16\pi^2\sigma^2 L^2 R^4)^{1/2}$ , and the primes indicate derivatives with respect to  $r$ . Time derivatives of lapse and shift do not appear in the action, which leads to the constraints  $\Pi_{N^t} = \Pi_{N_r} = 0$ . When imposed on the wave function, this leads to

$$\Psi = \Psi[L, R, q].$$

Derivative of the action with respect to lapse and shift gives the constraints  $\mathcal{H}_{t,r} = 0$ .

With the ansatz

$$\Psi = e^{iW(L,R,q)},$$

the WKB approximation is obtained from a solution of the Hamilton-Jacobi equations

$$\mathcal{H}_{t,r} \left( \frac{\partial W}{\partial L}, \frac{\partial W}{\partial R}, \frac{\partial W}{\partial q}, L, R, q \right) = 0.$$

We are interested in a solution which interpolates between suitable turning points.

Away from the source at  $r = q(t)$ , we may define

$$M(r) = \frac{G\Pi_L^2}{2R} + \frac{R}{2G} \left\{ 1 - \left( \frac{R'}{L} \right)^2 - \frac{\Lambda R^2}{3} \right\}, \quad (32)$$

and we have  $M' = -R'\mathcal{H}_t/L - G\Pi_L\mathcal{H}_r/RL = 0$ , where we have used the Hamiltonian constraints. This implies that  $M$  is constant for  $r \neq q$ . At the turning point geometries the momenta vanish,  $\Pi_L = 0$ , and one has

$$\left( \frac{dR}{dy} \right)^2 = 1 - \frac{2GM}{R} - \frac{\Lambda R^2}{3}, \quad (33)$$

where  $dy = Ldr$ . This is of course the relation between the intervals of proper length  $dy$  and proper radius of the 2-spheres  $dR$  in the Schwarzschild-(A)dS geometry (in static coordinates). We are mostly interested here in the case with  $M = 0$ , and with  $\Lambda > 0$ , where turning point geometries  $R_b(y)$  and  $R_a(y)$  before and after the tunneling will be the equatorial slices of the 4-sphere and of the domain-wall deSitter solution. The functions  $R_b(y)$  and  $R_a(y)$  are given by Eqs. (18) and (19) respectively.

From (32), we have

$$\Pi_L^2 = -\frac{R^2}{G^2} \left\{ 1 + V(R) - \left( \frac{R'}{L} \right)^2 \right\}, \quad (34)$$

where we have introduced

$$V(R) = -2GM/R - (\Lambda/3)R^2.$$

At the wall ( $r = q$ ), the constraints are consistent with  $L$  and  $R$  being continuous, while they imply the following discontinuities for  $\Pi_L$  and  $R'$ :

$$[\Pi_L] = -p/L, \quad [R'] = -GE/R. \quad (35)$$

[note that at the turning point, the first equation is trivial since the momenta vanish, and the second reproduces Eq. (10)]. Moreover, from Eq. (31) we have

$$\Pi_R = L \frac{\Pi_L'}{R'} + \frac{p}{R'} \delta(q - r), \quad (36)$$

which by virtue of (35) does not have delta-function contributions on the wall. Note that from (34) and (36) we can write  $\Pi_L$  and  $\Pi_R$  in terms of  $L(r)$  and  $R(r)$ . In particular

$$\Pi_R = \left( \frac{L}{R} + \frac{V'/2 - (R'/L)'}{1 + V - (R'/L)^2} \right) \Pi_L, \quad (37)$$

where  $V' \equiv dV(R)/dR$  and  $\Pi_L$  is given by (34). Also, the momentum  $p$  is determined by (35) in terms of  $L(r)$  and  $R(r)$  in the neighborhood of  $r = q$ .

The solution of the Hamilton-Jacobi equation  $W(L, R, q)$  satisfies

$$\delta W = p \delta q + \int (\Pi_L \delta L + \Pi_R \delta R) dr, \quad (38)$$

for arbitrary variations  $\delta q, \delta L(r)$  and  $\delta R(r)$ . Under the barrier, where  $R'^2 \leq L^2(1 + V)$ , we may define [14]

$$\Omega(L, R, q) = G^{-1} \int dr \left( RL \sqrt{1 + V - (R'/L)^2} - R R' \alpha \right), \quad (39)$$

where we have introduced the function

$$\alpha = \arccos \left( \frac{R'}{L \sqrt{1 + V}} \right). \quad (40)$$

Here, the inverse cosine is defined in the range  $0 \leq \alpha \leq \pi$  (so that the sine is positive). It is straightforward to check that under arbitrary variations of the arguments of  $\Omega$ , we have

$$\delta \Omega = \pm i \delta W - G^{-1} \int dr \frac{d}{dr} (\alpha R \delta R) + G^{-1} [R' \alpha] R \delta q. \quad (41)$$

The second term in the right hand side arises from partial integration in the variation with respect to  $R$ , and it is non-vanishing because  $R'$  is discontinuous across the wall. The square brackets in the last term indicate the discontinuity (that is, the quantity evaluated at  $r = q + \epsilon$  minus the quantity evaluated at  $r = q - \epsilon$ ). This term arises from variation with respect to  $q$  of the second term in (39) (variation of the first term in (39) produces the term  $\pm ip\delta q$ , which has been included in  $\pm i\delta W$ ). The last two terms in the right hand side of (41) only depend on quantities evaluated near the wall. Using  $d\hat{R} = \delta R + R'\delta q$ , where  $\hat{R} = R(r = q)$  is the proper radius of the wall, they can be combined into  $G^{-1}[\alpha]\hat{R}d\hat{R}$ . Hence, we have

$$\pm iW(L, R, q) = \Omega - G^{-1} \int [\alpha] \hat{R} d\hat{R}. \quad (42)$$

Since  $\alpha$  is a function which depends on  $R, R'$  and  $L$ , it may appear that the last integral cannot be done unless a semiclassical path is completely specified. However, the system is integrable, and  $[\alpha]$  can in fact be found from the discontinuities (35) in terms of  $\hat{R}$ . From Eqs. (34) and (40), we have

$$(R'/L) = \sqrt{1+V} \cos \alpha, \quad \Pi_L = \pm i G^{-1} R \sqrt{1+V} \sin \alpha. \quad (43)$$

It follows from (35) that

$$[\sqrt{1+V} \sin \alpha] = \pm i(Gp/LR), \quad [\sqrt{1+V} \cos \alpha] = -(GE/LR). \quad (44)$$

Squaring and adding both equations in (44), we immediately find

$$\cos[\alpha] \equiv \cos(\alpha_+ - \alpha_-) = \frac{2 + V_+ + V_- - (4\pi G\sigma\hat{R})^2}{2\sqrt{1+V_+}\sqrt{1+V_-}}, \quad (45)$$

where the subindices  $+$  and  $-$  refer to the limiting values on both sides of the wall. Note that  $V_+ = V(R(q + \epsilon))$  and  $V_- = V(R(q - \epsilon))$  can be different if the cosmological constants are different on both sides of the wall, or if the bubble configuration has non-vanishing mass  $M \neq 0$ . Eq. (44) determines  $[\alpha]$  in terms of  $\hat{R}$ , but only up to a sign. Since  $0 \leq \alpha_{\pm} \leq \pi$ , we have

$$\text{sign}[\alpha] = -\text{sign}[\cos \alpha] = -\text{sign}[R'/\sqrt{1+V}]. \quad (46)$$

In particular, we shall see in the Appendix that in the applications we are interested in, one of these two conditions are met: either we can construct a semiclassical path for which  $p = 0$ , or we can construct a semiclassical path for which  $V_+ = V_-$ . In both cases, it follows that

$$\text{sign}[\alpha] = \text{sign}E = \text{sign}\sigma. \quad (47)$$

We are interested in the change  $i\Delta W$  between the turning point geometries  $R_b$  and  $R_a$ ,

$$\pm i\Delta W = \Omega(R_a) - \Omega(R_b) - \int_{\hat{R}_b}^{\hat{R}_a} \frac{\text{sign}[\alpha]}{G} \arccos \left[ \frac{2 + V_+ + V_- - (4\pi G\sigma\hat{R})^2}{2\sqrt{1+V_+}\sqrt{1+V_-}} \right] \hat{R} d\hat{R}. \quad (48)$$

where it is now understood that the inverse cosine lies between 0 and  $\pi$ . The value of  $\Omega$  at the turning point geometries is easy to evaluate. The first term in the integrand of (39) vanishes, and in the second term  $\alpha = \pi\Theta(-R')$ , where  $\Theta$  is the step function. As noted in [14], the integral only receives contributions where the geometry is backtracking ( $R' < 0$ ), and the integral yields

$$\Omega = (\pi/2G)\Delta R^2, \quad (49)$$

where  $\Delta R^2$  is the absolute value of the change in  $R^2$  in the backtracking part of the geometry.

Let us now particularize the general formula (48) to the problem of nucleation of walls in deSitter space, where the turning point geometries are given by (18) and (19). For deSitter space

$$\Omega(R_b) = \frac{\pi}{2GH^2}. \quad (50)$$

For the nucleation of positive tension walls, the geometry backtracks from  $R_w$ , given by (21), to  $R = 0$ , and so

$$\Omega(R_a) = \frac{\pi R_w^2}{2G}, \quad (\sigma > 0). \quad (51)$$

On the other hand, for the nucleation of negative tension walls, we have two backtracking pieces. First from  $R = H^{-1}$  to  $R = R_w$ , and then from  $R = H^{-1}$  to  $R = 0$ . Both contribute and give rise to

$$\Omega(R_a) = \frac{\pi}{GH^2} - \frac{\pi R_w^2}{2G}, \quad (\sigma < 0). \quad (52)$$

In both cases, we have

$$\Delta\Omega = (\Omega_a - \Omega_b) = \frac{\pi}{2G}(R_w^2 - H^{-2}) \text{sign}\sigma. \quad (53)$$

The integral in (48) is taken between  $\hat{R}_b = 0$ , corresponding to a wall of infinitesimal size before tunneling, and  $\hat{R}_a = R_w$ . Also, since we are discussing the case where the cosmological constant outside and inside the wall are the same, and where the initial bubble has infinitesimally small mass, we have  $V_+ = V_- = -H^2\hat{R}^2$ . The third term in (48) becomes

$$\begin{aligned} \frac{-\text{sign}\sigma}{2GH^2} \int_0^{x_w} \arccos \left[ \frac{1 - (1 + 8\pi^2 G^2 \sigma^2 H^{-2})x}{1 - x} \right] dx = \\ \frac{-\pi}{4GH^2} [2\pi G\sigma R_w - (2\pi G\sigma R_w)^2 \text{sign}\sigma], \end{aligned} \quad (54)$$

where  $x_w = H^2 R_w^2 = H^2/[H^2 + (2\pi G\sigma)^2]$ . Adding (53) and (54), we have

$$\pm i\Delta W = -\frac{\pi^2 \sigma R_w}{H^2} = -\frac{1}{2}I_E \quad (55)$$

where  $I_E$  is given by Eq. (23) [or by Eq. (25)] for a positive [or negative] tension wall.



Eq. (48) applies also to the case of diwalls. In this case,  $V = 0$  and the calculation simplifies somewhat. The turning point before tunneling is given by a flat three dimensional space  $R_b(y) = y$ , whereas the turning point after tunneling is given by Eq. (12). The first and second terms in the right hand side of (48) can still be calculated from (49). The flat space has no backtracking part, as  $R_b$  is monotonic, and doesn't contribute, whereas for the turning point after tunneling we have

$$\frac{\pi}{2G}\Delta R^2 = \frac{1}{8\pi G^3}(\sigma_1^{-2} - \sigma_2^{-2}).$$

The third term in the right hand side of (48) includes a separate contribution from each one of the walls, which is readily calculated and contributes minus one half of the previous terms. Thus, we find

$$\pm i\Delta W = \frac{1}{16\pi G^3}(\sigma_1^{-2} - \sigma_2^{-2}) = -\frac{1}{2}I_E, \quad (56)$$

where now  $I_E$  is given by (15).

Thus, both for diwalls nucleating in flat space and for walls (ghost or ordinary) nucleating in deSitter, the WKB "suppression factor" is given by

$$e^{-2|\Delta W|} = e^{-|I_E|}. \quad (57)$$

In the next Subsection we shall further elaborate on the relation between the Euclidean action and the tunneling rates in general.

Note that, since the system is integrable, the precise form of the semiclassical path has not been used in deriving (48) (except in determining the sign of  $[\alpha]$ , see the discussion around Eq. (47)). In the Appendix, we construct a WKB tunneling path for the cases discussed in this subsection. The trajectories considered are such that the radii of the walls grow monotonically from an infinitesimally small size to the turning point size  $R_w$ . It is interesting to note, in particular, that for the case of creation of negative tension walls in deSitter, the deformation of the geometry is smooth and the three volume is never zero (This is in contrast with the instanton picture where the deSitter geometry first disappears and then reappears with a large bubble in it). Note also that, due to the change in topology, we do not have the possibility of constructing a semiclassical path for the case of nucleation of negative tension walls in exactly flat space. Physically, this seems to be in agreement with the fact that the tunneling suppression for nucleation of such objects in deSitter becomes insurmountable in the limit  $H \rightarrow 0$ .

## 2.5 The Euclidean action and the tunneling rates

Eq. (57) suggests that given a semiclassical path with Euclidean action  $I_E$ , the corresponding tunneling rate is given by

$$\Gamma \sim e^{-2|\Delta W|} = e^{-|I_E|}. \quad (58)$$

For systems with a single degree of freedom, the tunneling suppression is indeed given by  $e^{-2|\Delta W|}$ . However, for loosely bound systems of ordinary and ghost matter, the situation is not so clear, and the above formula need not be of general validity.

To illustrate this point, let us consider the Euclidean solution corresponding to the nucleation of diwalls in flat space, considered in Subsection 2.1. We may in fact study the analogous solution in the presence of a cosmological constant. It is straightforward to show that the corresponding Euclidean action is given by

$$I_E^{diwall}(\sigma_1, \sigma_2, H) = I_E^+(\sigma_1, H) + I_E^-(\sigma_2, H) \quad (59)$$

where  $I_E^\pm$  are the actions for nucleation of positive and negative domain walls in deSitter, given by Eqs. (23) and (25). Note that, since  $I_E^+$  and  $I_E^-$  have opposite sign, we have

$$|I_E^{diwall}(\sigma_1, \sigma_2, H)| < |I_E^+(\sigma_1, H)| + |I_E^-(\sigma_2, H)|. \quad (60)$$

This means that if Eq. (58) is valid, it should be easier to form a diwall, than it is to create a wall of negative tension and then, subsequently, another wall of positive tension. Is this a reasonable expectation?

A simple system which bears a useful analogy with the system of diwalls is that of an electron and a proton crossing an electric barrier. Consider a one-dimensional barrier (fig. 5) where from left to right, the electric field  $-E$  is negative in a segment of width  $d_-$ , vanishing in a large segment of length  $L$ , and positive with strength  $+E$  in a third segment of width  $d_+ > d_-$ . A proton of very low kinetic energy impinging from the left bounces off the first segment, repelled by the electric field. The probability for it to go through the barrier is exponentially small, and practically vanishing in the limit of large  $L$ . Likewise, an electron of very low kinetic energy has no trouble going through the first two segments of the barrier, but will never make it to the asymptotic region on the right since it simply doesn't have enough energy. On the other hand, if the proton and electron are bound together, the resulting hydrogen atom has no trouble going through the barrier. The electron pulls the proton through the negative electric field, and the proton pulls the electron through the third segment with positive electric field.

Going back to the system of diwalls, let us first consider the limit  $H \ll G\sigma$ , when the Hubble radius is much larger than the scale characterizing the gravitational field of the walls. In this limit, the walls can be thought as a tightly bound system. In flat space ( $H \rightarrow 0$ ) both

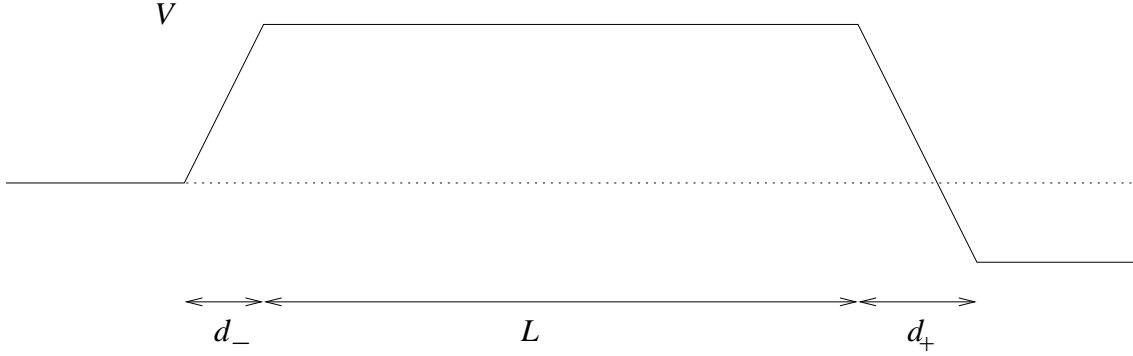


Figure 5: Electric potential barrier exemplifying how a bound system can behave very differently than its constituents in a tunneling process. The probability that a proton tunnels through this potential is negligible for large  $L$ . An electron feels an inverted potential, and if its energy is small enough it cannot appear as an asymptotic state in the region to the right. However, a hydrogen atom can easily cross the barrier as long as it is not ionized by the electric field. Similarly, a diwall, or a pair of Bondi dipoles, can be nucleated out of empty space if the normal and ghost constituents are tightly bound by gravity, even if their separate nucleation rates are strongly suppressed.

$I_E^+$  and  $I_E^-$  diverge. Physically, it is impossible to nucleate either a positive energy wall or a negative energy wall in Minkowski. Separately, both processes would lead to a breakdown of energy conservation (barring the possibility of topology change). Yet, the diwall process seems to be possible and it should occur at a finite rate. The two walls push and pull each other through a barrier which none of them would be able to penetrate separately. In this sense, it is not surprising that Eq. (58) gives a higher probability to nucleation of diwalls than to the separate nucleation of walls of either tension.

On the other hand, in the limit  $G\sigma \ll H$  the gravitational field of the walls (and their interaction) becomes negligible. In this limit, the walls can be treated as non-gravitating objects in the background external field of a fixed deSitter space. The instanton for nucleation of walls of positive or negative tension is just a maximal worldsheet 3-sphere of radius  $H^{-1}$  embedded in  $S^4$ . The corresponding action is  $I_E^\pm \approx \pm 2\pi^2 \sigma H^{-3}$ . The action for the diwall is  $I_E^{diwall} \approx 2\pi^2(\sigma_1 - \sigma_2)H^{-3}$ , and in the limit when the positive and negative tension walls have approximately the same modulus,  $\delta\sigma/\sigma \ll 1$ , we have  $|I_E^{diwall}| \ll |I_E^+| + |I_E^-|$ . Eq. (58) would suggest that if  $\delta\sigma \ll H^3$ , diwall production is unsuppressed, even if  $\sigma \gg H^3$ . However, this cannot be true, since in the limit we are considering the interaction between walls is negligible. Production of walls (and diwalls) should be suppressed, with an exponent which is parametrically of order  $\sigma/H^3$ . In the example of the proton and electron crossing an electric barrier, this limit of weakly bound components would correspond to the case when there is a thermal bath of temperature  $T \gtrsim V_0$ , where  $V_0$  is the ionization energy, or when

the electric field is intense enough to ionize the atom  $Er_b \gtrsim V_0$ , where  $r_b$  is the Bohr radius. In both cases, the proton cannot get hold of the electron, and both have to go through the barrier on their own, so tunneling is highly suppressed.

The above examples suggest that Eq. (58) is a good estimate of the nucleation rate only in the case when we have a tightly bound system of ghosts and ordinary matter. However, it overestimates the rate when the gravitational binding energy between ghost and matter components is weak compared to any other force involved in the tunneling (*e.g.*, the expansion of the universe caused by  $\Lambda$  in the case of wall production in deSitter, the difference in pressure on both sides of the wall if we consider simultaneous false vacuum decay in ghost and matter sectors, or the electric force if we consider the Schwinger process occurring simultaneously in both sectors). In the general case, Eq. (58) is at best a conservative upper bound to the nucleation rate.

In the following sections, we shall be interested in nucleation of lumps of ghost and ordinary matter in flat space. In this case, the system can be considered to be tightly bound, since the gravitational energy-momentum transfer between matter and ghosts is what allows the system to nucleate (there is no other driving force). In the light of the above discussion, we shall adopt Eq. (58) as our estimate for the nucleation rate. Investigation of the general case of weakly bound systems is left for further research.

### 3 Nucleation of Bondi dipoles

We now turn to discussing the spontaneous nucleation of particle-like ghosts, accompanied with ordinary particles.

#### 3.1 Preliminaries

A spherically symmetric lump of neutral ghost matter of mass  $m < 0$  coupled to non-ghost gravity creates the gravitational field

$$ds^2 = - \left( 1 + \frac{2G|m|}{\rho} \right) dt^2 + \frac{d\rho^2}{\left( 1 + \frac{2G|m|}{\rho} \right)} + \rho^2 d\Omega^2. \quad (61)$$

This metric exhibits a naked singularity at  $\rho = 0$ . This singularity is usually regarded as a ‘valuable’ one [15], *i.e.*, one not to be regularized since it signals a pathological negative-energy spectrum unbounded below. However, here we intend to explore how deadly this pathology is. So we assume that (61) is a valid description of the gravitational field, though only down to distances of the order of the gravitational cutoff distance scale  $1/\mu$ , or, for a light ghost lump  $|m| < \mu$ , down to the Compton wavelength  $1/|m|$ .

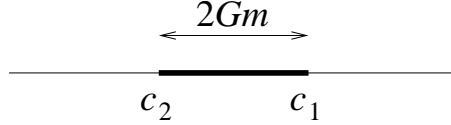


Figure 6: Axisymmetric Weyl solutions are specified by giving the sources along the axis for the ‘potential’  $U$ . The Schwarzschild solution corresponds to an infinitely thin rod of linear density  $+1/2$  and length  $2Gm$ .

We are interested in configurations with several collinear ghost and normal particles. The class of metrics that describes these are the axisymmetric Weyl solutions

$$ds^2 = -e^{2U} dt^2 + r^2 e^{-2U} d\phi^2 + e^{2(\nu-U)} (dr^2 + dz^2) \quad (62)$$

where  $U$  and  $\nu$  are functions of  $r$  and  $z$ . This is a well-studied system (see *e.g.*, [16]) so we shall only sketch its solution. The vacuum Einstein equations can be completely integrated in an explicit form: the function  $U$  satisfies a Laplace equation in the auxiliary space  $dr^2 + dz^2 + r^2 d\phi^2$ , and then  $\nu$  can be obtained from  $U$  by quadratures. Hence the solutions are fully determined once we specify the sources for the axisymmetric potential  $U$ . For example, the Schwarzschild solution with positive mass  $m$  corresponds to taking as a source an infinitely thin rod of length  $2Gm$  and linear mass density  $1/2$  along the  $z$  axis (fig. 6), so

$$e^{2U} = \frac{X_2}{X_1} \quad (63)$$

and

$$e^{2(\nu-U)} = \frac{Y_{12}}{4R_1 R_2}, \quad (64)$$

where we introduce notation that is useful for this class of solutions [17],

$$R_i = \sqrt{r^2 + (z - c_i)^2}, \quad (65)$$

$$X_i = R_i - (z - c_i), \quad (66)$$

$$Y_{ij} = R_i R_j + (z - c_i)(z - c_j) + r^2, \quad (67)$$

and, for this particular solution,  $c_1 - c_2 = 2Gm$ . It may seem odd that the spherically symmetric Schwarzschild solution is obtained from a non-spherical source, but this is just an artifact of the Weyl representation. The rod at  $r = 0$ ,  $c_2 < z < c_1$ , in fact corresponds to the Schwarzschild horizon, and it is possible to see in general that a regular horizon is present iff the rod density is  $1/2$ , otherwise a naked singularity will appear. In this paper, however, we will only consider situations where the geometry is cutoff before the horizon (or the naked singularity) is reached.



Figure 7: Left: the source for a ghost particle of mass  $-m_-$  is a rod of length  $2Gm_-$  and linear density  $-1/2$  (dotted rod). This can be obtained from eqs. (63)-(64) by simply taking  $c_1 < c_2$ . Right: the C-metric describing accelerating black holes corresponds to a finite rod for the black hole, and a semi-infinite rod for the acceleration horizon. Weyl coordinates cover only one Rindler wedge of the entire spacetime.

The field of a ghost particle (61) is given by a configuration similar to the one above, but now the density of the rod is instead  $-1/2$ . A simple way to obtain this from the solution (63)-(64) is to take  $c_1 < c_2$ , with  $c_2 - c_1 = 2G|m|$ . For definiteness and simplicity we shall only consider normal and ghost particles with rod linear densities  $\pm 1/2$ —other densities do not introduce any significant qualitative changes.

It is now easy to construct axisymmetric configurations with arbitrarily many collinear particles. One simply superposes rods corresponding to each of the particles.  $U$  is then the linear superposition of the fields of each rod, and then the function  $\nu$  can be explicitly integrated [8, 17, 18]. Of course, in general the particles will attract each other (or possibly repel if ghosts are present) so there will be uncanceled forces among the particles. This reflects itself in the geometry through the presence of conical singularities on the portions of the  $z$ -axis away from the rods. For Weyl metrics (62), the conical deficit angle  $\delta$  at a given point  $z_0$  on the axis away from any rod, is given by

$$2\pi - \delta = \lim_{r \rightarrow 0} \frac{2\pi}{\sqrt{g_{rr}}} \frac{d\sqrt{g_{\phi\phi}}}{dr} \Big|_{z=z_0} = 2\pi \lim_{r \rightarrow 0} e^{-\nu} \Big|_{z=z_0} . \quad (68)$$

A conical *deficit* angle  $\delta > 0$  on a certain segment of the axis can be interpreted as a string stretched along the segment and pulling together the objects at its endpoints, while a conical *excess* angle  $\delta < 0$  is a strut pushing the objects apart. An integration constant in  $\nu$  (corresponding to constant rescalings of  $\phi$ ) can be used to eliminate possible conical singularities on a given segment, but in general, once this is fixed, there will remain conical singularities at other segments. In some cases it will be possible to tune parameters in the solution to cancel all conical singularities: the system is then balanced. If it is impossible to cancel all of them, then external forces are needed to keep the configuration in place.

Finally, we note that a semi-infinite rod of density  $+1/2$  corresponds to an acceleration horizon. The Weyl coordinates cover in this case only a Rindler wedge of the whole spacetime, but they can be extended across the Rindler horizon to provide a maximal analytic extension of the geometry, which contains a second copy of the Rindler wedge [8, 9]. For instance, the configuration corresponding to a finite, positive mass rod, and a semi-infinite rod, is known

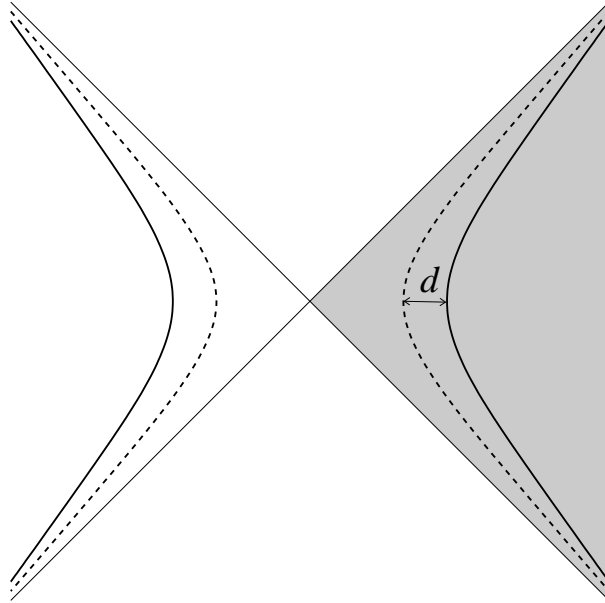


Figure 8: A pair of Bondi dipoles accelerating apart. Weyl coordinates cover only one wedge (shaded) of the full spacetime, containing a single Bondi dipole. A normal particle (solid worldline) is chased by a ghost (dotted worldline). The dipoles self-accelerate away with uniform acceleration, and the configuration is boost-invariant.

as the C-metric (see fig. 7) and describes two black holes accelerating away with uniform acceleration, each in a separate Rindler wedge, and being pulled apart by strings [19, 20].

### 3.2 Accelerating Bondi dipoles

A Bondi dipole consists of a positive and a negative mass particle [7]. If we construct the gravitational field of this configuration as the Weyl metric for a positive density and a negative density rod, and nothing else, then it is straightforward to see that no choice of the rod parameters is able to cancel all conical singularities on all segments of the axis away from the rods. In particular, if we eliminate the conical defects at infinity, then a strut remains inbetween the two particles. This is of course expected, since the two particles can not remain in static equilibrium. The strut pushes the normal particle away from the ghost, while the ghost is also pushed away, but having negative mass, it will tend to accelerate in a direction opposite to the one it is pushed in<sup>2</sup>. This indicates that the Bondi dipole will naturally accelerate together, the ghost chasing after the normal particle in a runaway fashion.

---

<sup>2</sup>Hence Gamow’s term “donkey particle” for such ghosts [21].

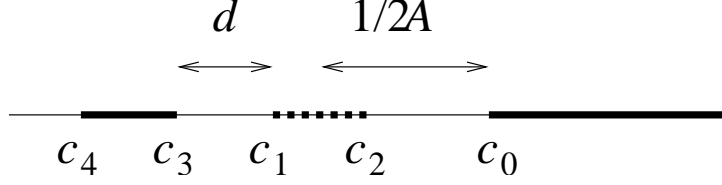


Figure 9: Weyl sources for an accelerating Bondi dipole: a ghost particle (negative density rod at  $c_1 < z < c_2$ ) chases a normal particle (positive density rod at  $c_4 < z < c_3$ ). The maximally extended solution contains a second pair accelerating in the opposite direction.

From our previous discussion, it should be obvious how to construct the Weyl metric for such a configuration<sup>3</sup>. From left to right, take the sources for the potential  $U$  to be (figure 9): a semi-infinite rod at  $z > c_0$  (and of density  $+1/2$ ) for the acceleration horizon; a negative density rod at  $c_1 < z < c_2 < c_0$  for the ghost; and a positive density rod at  $c_4 < z < c_3 < c_1$  for the normal particle. Note that again we have chosen to label the rod endpoints  $c_i$  in such a way that the conventional correlative order is inverted for the negative density rod, *i.e.*, we take  $c_1 < c_2$ . This is done in order to facilitate a direct comparison to the solution in [17], which described two normal particles (black holes) accelerating together. Then we can directly read off our solution from [17] as

$$\begin{aligned} e^{2U} &= A_- \frac{X_0 X_2 X_4}{X_1 X_3}, \\ e^{2(\nu-U)} &= \frac{Y_{01} Y_{12} Y_{03} Y_{34} Y_{14} Y_{23}}{8 A_- R_0 R_1 R_2 R_3 R_4 Y_{02} Y_{04} Y_{13} Y_{24}} \end{aligned} \quad (69)$$

with

$$c_4 < c_3 < c_1 < c_2 < c_0, \quad (70)$$

and  $A_-$  a constant with dimension of inverse length whose value can be changed by coordinate rescalings. For later convenience we choose it as

$$A_-^{-1} = 2c_0 - c_1 - c_2. \quad (71)$$

The inversion in the ordering between  $c_1$  and  $c_2$  in (70) compared to [17] changes a positive mass into a negative one. Note also that we can always perform a shift in  $z$  to fix one of the  $c_i$ , so the solution contains only four physical parameters. To identify the physical

---

<sup>3</sup>A slightly different version of the Bondi dipole was constructed in [9], with point-like sources for the normal and ghost particle. These are then “Chazy-Curzon particles”. For our purposes, the qualitative properties are basically the same as in our solution. In particular, the result for the action of the corresponding instanton takes the same form as in eq. (87). Other instances of self-accelerating positive+negative mass bound states are discussed in [22].



quantities, we take the approximation where the rods are well separated from each other, and the dipole has a size smaller than the acceleration length scale, *i.e.*,

$$c_3 - c_4 \sim c_2 - c_1 \ll c_1 - c_3 \ll c_0 - c_2, \quad (72)$$

so the gravitational forces between the particles involved are weak. A careful examination of the solution in different limits then allows to identify<sup>4</sup>

$$\begin{aligned} m_+ &= \frac{c_3 - c_4}{2G} \frac{A_+}{A_-}, & m_- &= \frac{c_2 - c_1}{2G}, \\ A_+^{-1} &= \sqrt{\frac{2c_0 - c_3 - c_4}{A_-}}, & d &= c_1 - c_3. \end{aligned} \quad (73)$$

All these quantities are invariant under shifts along the  $z$  axis. The approximation (74) is now equivalent to

$$Gm_+ \sim Gm_- \ll d \ll A_-^{-1} \sim A_+^{-1}, \quad (74)$$

and in this limit we can approximately interpret  $m_+$ ,  $A_+$  and  $-m_-$ ,  $A_-$ , respectively, as the masses and accelerations of the positive and negative particles, and  $d$  as the distance between them. In particular, in the approximation (74) the harmonic difference of accelerations satisfies (see figure 8)

$$\frac{1}{A_+} - \frac{1}{A_-} \simeq d. \quad (75)$$

Note that with our definition,  $m_-$  is positive, so the ghost mass is  $-m_-$ . We can take the four physical parameters of the solution to be  $m_{\pm}$ ,  $d$  and  $A_-$ , while  $A_+$  is fixed in terms of them.

In (69) we have already fixed the integration constant in  $\nu$  so as to have

$$\lim_{r \rightarrow 0} e^{-\nu}|_{(z < c_4)} = 1 \quad (76)$$

and therefore, according to (68), there is no conical defect at infinity as long as  $\phi \sim \phi + 2\pi$ . On the other hand, at the segment inbetween the two rods we have

$$\lim_{r \rightarrow 0} e^{-\nu}|_{(c_3 < z < c_1)} = \frac{(c_0 - c_3)(c_2 - c_3)(c_1 - c_4)}{(c_1 - c_3)(c_0 - c_4)(c_2 - c_4)} \quad (77)$$

and between the ghost rod and the acceleration horizon,

$$\lim_{r \rightarrow 0} e^{-\nu}|_{(c_2 < z < c_0)} = \frac{(c_0 - c_1)(c_0 - c_3)}{(c_0 - c_2)(c_0 - c_4)}. \quad (78)$$

---

<sup>4</sup>These identifications are not uniquely determined: they can be modified by terms that are small in the limit (74). Our choices simplify some expressions below.

To cancel conical singularities on all segments we must require equality of (76), (77), (78), *i.e.*,

$$\frac{(c_2 - c_3)(c_1 - c_4)}{(c_1 - c_3)(c_2 - c_4)} = \frac{c_0 - c_1}{c_0 - c_2} = \frac{c_0 - c_4}{c_0 - c_3}. \quad (79)$$

The conditions (79) leave only two free parameters in the solution, which we could take to be the two masses  $m_+$ ,  $m_-$ , of the dipole constituents. In that case, the size and acceleration of the dipole would be fixed.

After some algebra and using the definitions (73), the second equality in (79) can be exactly recast into the form of Newton's third law

$$m_+ A_+ = m_- A_- . \quad (80)$$

Since necessarily we have  $A_+ < A_-$ , this implies that

$$m_+ > m_- . \quad (81)$$

This requirement will be important later on.

Also, in the approximation of weak fields (74), the conditions (79) become

$$\frac{Gm_+m_-}{d^2} \simeq m_- A_- = m_+ A_+ , \quad (82)$$

which reproduce Newton's force law, as expected. Finally, in this approximation eqs. (79) imply

$$m_+ - m_- \equiv \Delta m \simeq \frac{Gm_+m_-}{d} . \quad (83)$$

Hence the relative difference between the (absolute values of the) masses of the two components of the dipole is small relative to their masses.

### 3.3 Pair creation of Bondi dipoles

If we analytically continue the solution of the previous subsection to imaginary time, we obtain a Euclidean instanton where the dipole runs in a loop, with Euclidean time playing the role of the angle coordinate in the loop. Since the solution is asymptotically flat, the initial state is the Minkowski vacuum, which then tunnels to a zero-energy configuration with two Bondi dipoles self-accelerating away in opposite directions. This decay of the Minkowski vacuum is the non-perturbative analogue of the process (3),

In order to compute the Euclidean action  $I_E$ , we follow [23]. The periodicity of Euclidean time is fixed by requiring regularity at the Rindler horizon only —we are assuming that the normal particle has no horizon. As long as we assume that the region near the ghosts is smoothed out by ghost matter fields that satisfy the classical Einstein equations, we do not

need to know the details of how the naked singularity is avoided—nor how normal matter modifies the geometry to avoid the black hole horizon. Bulk terms in the action (including matter and ghost fields) vanish on-shell, and only boundary terms contribute. These are entirely given in terms of the gravitational field. The action contains a contribution from the Hamiltonian, which vanishes for this zero-energy configuration, plus terms arising from the horizons. We are assuming that the positive mass particles possess no black hole horizons, so the only contributions come from the acceleration horizons. The action is then

$$I_E = -\frac{\Delta\mathcal{A}}{4G} \quad (84)$$

where  $\Delta\mathcal{A} = \mathcal{A}^{(f)} - \mathcal{A}^{(i)}$  is the difference between the areas of the acceleration horizons after and before the nucleation process, *i.e.*, in the instanton and in the reference Minkowski background. Each of these is evaluated as

$$\mathcal{A} = \int d\phi \int_{c_0}^{z_{\max}} dz \sqrt{g_{zz}g_{\phi\phi}}|_{r=0} . \quad (85)$$

Since the area of acceleration horizons is infinite, we have regularized them with a long distance cutoff  $z_{\max} \gg c_0$ . In general  $z_{\max}^{(f)} \neq z_{\max}^{(i)}$ , and in order to make sure that the subtraction is correctly performed, one must match the lengths of the two acceleration horizons

$$\ell = \int d\phi \sqrt{g_{\phi\phi}}|_{r=0, z=z_{\max}} . \quad (86)$$

Imposing  $\ell^{(f)} = \ell^{(i)}$  fixes the relation between the long-distance cutoffs  $z_{\max}^{(i)}$  and  $z_{\max}^{(f)}$ . For finite cutoffs, the two areas are finite and we can compute their difference. Finally, removing the regulators leaves a finite non-zero result

$$I_E = \frac{\pi}{2GA_-}(c_1 - c_2 + c_3 - c_4) = \pi \left( \frac{m_+}{A_+} - \frac{m_-}{A_-} \right) . \quad (87)$$

As an aside, we note that this result can be easily generalized to configurations with arbitrarily many accelerating particles and ghosts. If the finite rods (of density  $\pm 1/2$ ) have endpoints at  $z = c_i$ , then the contribution to the action coming from  $\Delta\mathcal{A}$  is of the form  $\frac{\pi}{2AG} \sum_i \pm c_i$ , where the sign for  $c_i$  is positive (negative) if the density along the axis increases (decreases) as we go from right to left at  $z = c_i$ . If we identify the masses and accelerations with appropriate generalizations of (73), then this contribution to the action is equal to  $\pi \sum_i \pm \frac{m_i}{A_i}$ , where ghosts contribute with a minus sign.

Of course, the requirement of balance of forces (*i.e.*, absence of conical singularities) imposes relations between the parameters. Coming back to our example of the Bondi dipole, the condition (81) together with  $A_+ < A_-$  imply that the action (87) is always positive and

the decay rate is exponentially suppressed. In the weak field approximation the result reduces to

$$I_E \simeq 2\pi m_+ d \simeq \frac{\Delta m}{T_R}, \quad (88)$$

where the Rindler temperature is  $T_R = A_+/2\pi$ . The rate of the non-perturbative version of the decay (3) is therefore

$$\Gamma \sim e^{-2\pi m_+ d}. \quad (89)$$

## 4 Materialization of ghost couples

### 4.1 Ghost pairs in Minkowski space

Can we also find a non-perturbative analogue of the decay process (6), in which no normal particles are produced? Since (6) involves the creation of gravitons, non-perturbatively the decay might not only produce gravitational waves but also change significantly the final geometry. We shall show that this is indeed the case, and that the Minkowski vacuum undergoes a topology change.

We expect the solution that describes the decay to involve two ghost particles accelerating away from each other. In the terminology of the Weyl solutions discussed above, this should correspond to a semi-infinite rod for the acceleration horizon, and a finite rod of negative density for the ghost particle. From our Newtonian estimates in the introduction section, the two particles should be very close,  $r \sim Gm_-$ , *i.e.*, very close to the acceleration horizon. Therefore a strong gravitational backreaction is expected.

A simple way to construct this solution is to start from the configuration in the previous section (eq. (69) and fig. 9) and remove from it the normal particle, *i.e.*, the positive density rod, by setting  $c_3 = c_4$ . This leaves only the ghost particle in the Rindler wedge covered by these coordinates (its anti-ghost is in the opposite wedge). We must examine, though, the condition for balance of forces in this new configuration. With our choice of parameters no conical singularity is present at  $z < c_1$  (*i.e.*, out to infinity), but, if  $c_3 = c_4$ , it is impossible to eliminate the conical defect (78) at  $c_2 < z < c_0$ . The way around this, however, is to take  $c_2 \rightarrow c_0$ , hence eliminating the troublesome segment of the axis. In terms of the ‘physical’ parameters (71), (73), this implies

$$2Gm_-A = 1. \quad (90)$$

(from now on we drop the subindex  $-$  from  $A_- \rightarrow A$ ). Clearly, this means we are in a regime of strong self-gravity, so the interpretation of  $m_-$  as the ghost mass should not be taken any strictly.



Figure 10: Weyl sources for ghost and anti-ghost accelerating apart (the anti-ghost lies in the opposite Rindler wedge obtained by maximally extending the solution).

The Weyl form is rather unwieldy if one wants to study in detail the properties of this configuration. To get a better understanding of the geometry, it is more convenient to note that this solution is in fact a special case of the neutral C-metric of [19] (figure 7-right), namely, one with a particular negative value for the mass parameter. We then use a more conventional set of coordinates (see fig. 11-upper), in which the solution becomes

$$ds^2 = \frac{1}{A^2(x-y)^2} \left[ G(y)d\hat{t}^2 + (1+2Gm_-A)^2 \left( -\frac{dy^2}{G(y)} + \frac{dx^2}{G(x)} \right) + G(x)d\phi^2 \right], \quad (91)$$

where we use the form for the cubic function  $G(\xi)$  advocated in [24],

$$G(\xi) = (1 - \xi^2)(1 - 2Gm_-A\xi). \quad (92)$$

The change of coordinates between  $(r, z)$  and  $(x, y)$  can be found in [24]. The time coordinate  $t$  used in the Weyl form of the metric has, for convenience, been rescaled to  $\hat{t} = t \frac{A}{1+2Gm_-A}$ . Note we have not imposed the condition (90) yet. It will be rederived shortly.

The coordinate range is  $-\infty < y < -1$  and  $-1 \leq x \leq 1$ , with  $y \rightarrow x \rightarrow -1$  corresponding to asymptotic infinity. The acceleration horizon lies at  $y = -1$ .

For our purposes here, the axes of  $\phi$ , which lie at  $x = \pm 1$ , are of paramount importance. The surfaces at constant  $\hat{t}$  and constant  $y > -\infty$ , are, up to a conformal factor, described by

$$(1+2Gm_-A)^2 \frac{dx^2}{G(x)} + G(x)d\phi^2. \quad (93)$$

As long as  $2Gm_-A < 1$ , the function  $G(x)$  has simple zeroes at  $x = \pm 1$ . The coordinate  $x$  can be regarded as roughly similar to  $\cos \theta$  on  $S^2$ , so these surfaces are topological two-spheres enclosing the ghost particle, and  $x = \pm 1$  are the poles of the spheres. It is easy to see that if we identify  $\phi \sim \phi + 2\pi$ , then there is no conical defect at  $x = -1$ , *i.e.*, extending out to infinity. There is, though, a conical excess at the other pole  $x = +1$ , which stretches from the ghost towards the acceleration horizon, and thence to the anti-ghost. It is easy to see that this conical excess cannot be eliminated by any choice of parameters — just like we already found using the Weyl form of the solution. However, if we impose the condition (90), then the topology of these surfaces changes. Now the function

$$G(x) = (1-x)^2(1+x) \quad (94)$$

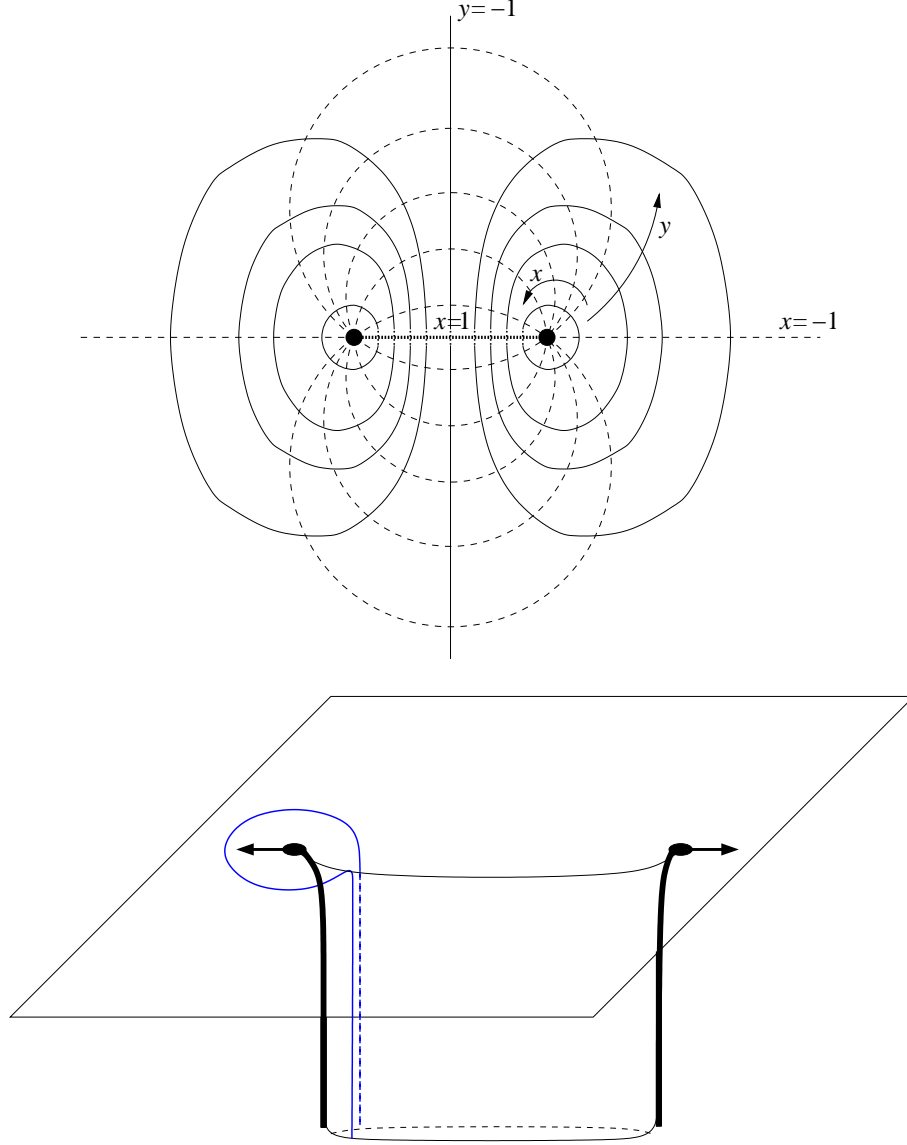


Figure 11: Section at  $t = 0$  (with the angular direction  $\phi$  suppressed) of the geometry with a pair of ghost particles. The upper figure sketches the coordinate system: solid lines are constant  $y \in (-\infty, 1]$ , dashed lines are constant  $x \in [-1, 1)$ . The lines (actually surfaces) at constant  $y$ , which surround the ghost singularity at  $y = -\infty$ , do not quite close at the axis  $x = 1$ , which lies an infinite spatial distance away. This corresponds to the infinite throat that stretches between the particles, sketched in the lower figure by taking a slanted view. A surface at constant  $y$  (depicted as a line) surrounding the ghost can be described as a sphere with an infinite funnel at one of its poles (so it is topologically  $\mathbb{R}^2$ , instead of  $S^2$ ). Since the ghosts are lumps that spread out to some finite  $y$  away from the singularity, they actually extend all the way down the throat. The surface  $y = -1$  is an acceleration horizon, so the two particles are causally separated.

has a double zero at  $x = 1$ . As a result, the singularity at  $x = 1$  is pushed an infinite spatial distance away, so it is removed from the spacetime. The coordinates  $(x, \phi)$  parametrize now a surface with topology  $\mathbb{R}^2$ , instead of  $S^2$ . Geometrically it is a sphere with an infinite funnel at one of its poles (figure 11-lower). Down the funnel at  $x \rightarrow +1$  it is convenient to introduce a new coordinate

$$\zeta = -\log(1 - x) \quad (95)$$

in terms of which the geometry (93), when the condition (90) holds, approaches

$$2(d\zeta^2 + e^{-2\zeta}d\phi^2) \quad (96)$$

with  $\zeta \rightarrow \infty$ : the tip of the funnel recedes to infinity as its width shrinks.

Thus the effect of choosing the parameters to satisfy (90) is to create an infinite throat that extends between the ghost and anti-ghost. Away from the naked singularities at the position of the ghosts ( $y \rightarrow -\infty$ ), the geometry is regular. Down the throat, when  $x \sim +1$ , and within the Rindler wedge  $-\infty < y \leq -1$ , the solution can be approximated by

$$ds^2 \simeq \frac{1}{A^2(1-y)^2} \left[ G(y)dt^2 - 4\frac{dy^2}{G(y)} + 2(d\zeta^2 + e^{-2\zeta}d\phi^2) \right]. \quad (97)$$

The size of  $\phi$ -circles at constant  $x$  goes from zero at the position of the ghost,  $y \rightarrow -\infty$ , to a maximum at the midpoint  $y = -1$ .

Figure 11 also reflects one peculiarity of this construction. Even though we have been referring to the singularities in this metric as ghost particles, the fact is that they are qualitatively different from the ones in (61). In particular, and in contrast to the ghosts in the Bondi dipole of the previous section, there is no limit of this solution where one recovers the single ghost solution (61). Then it becomes doubtful whether the ghost singularities in this solution, which are more string-like than particle-like, can be identified as localized “lumps of ghost matter”. This caveat should be borne in mind throughout our discussion.

As the ghost and antighost accelerate away, the infinite throat inbetween them grows. We can study the geometry at asymptotically late times using methods similar to those employed in [25]. First, note that asymptotic future lies in the upper wedge of the spacetime. To describe this region, we take  $y > -1$ , *i.e.*, we cross the Rindler horizon towards the future, extending the solution in the standard manner. Since in this region  $G(y) > 0$ , we now have  $y$  as the timelike coordinate, while  $t$  is spacelike. This means that the geometry in this region is time-dependent.

The range of coordinates that describes this “upper wedge” portion of spacetime is  $-1 \leq y < x \leq 1$ . There is no singularity in this region. Asymptotic future is approached as  $y \rightarrow x \rightarrow 1$  with  $y < x$ . In this limit the throat stretches out to infinity as the two particles fly away. To describe the resulting geometry when the ghosts are far away, consider

$1 - x \ll x - y \simeq 1 - y$ , and introduce, besides (95), new coordinates that measure proper distance and time

$$w = \frac{\sqrt{2}}{A} \hat{t}, \quad \tau = \frac{\sqrt{2}}{A(1-y)} \quad (98)$$

(recall  $\hat{t}$  is spacelike and  $y$  is timelike in the upper wedge). The spacetime in the aftermath of the decay is then

$$ds^2 \rightarrow -d\tau^2 + \tau^2 (d\zeta^2 + e^{-2\zeta} d\phi^2) + dw^2 \quad (\text{asymptotic future}). \quad (99)$$

It is now apparent that this is flat space: besides the flat coordinate  $w$  (which was Rindler time  $\hat{t}$  in the Rindler wedge) the rest of the spacetime is the three-dimensional Milne universe, which is locally flat. The Milne universe is an open ( $k = -1$ ) FRW universe with spatial sections of constant negative curvature. Note, however, that in the spatial sections in (99) there is no need *a priori* to impose any periodicity requirements on  $\phi$ , since  $\partial_\phi$  does not have any fixed-points at finite spatial distance. But, since this is an extension of the solution from the Rindler wedge, we *must* have the same periodicity for  $\phi$  on both sides of the Rindler horizon, *i.e.*,  $\phi \sim \phi + 2\pi$  also in (99). Although locally the geometry is unaffected, these identifications change the spatial sections of the Milne universe from a hyperboloid of topology  $\mathbb{R}^2$  to an infinite funnel of topology  $\mathbb{R} \times S^1$ , the former being the universal covering of the latter.

To summarize, the non-perturbative production of a pair of ghosts makes flat spacetime undergo a topology change from  $\mathbb{R}^{1,3}$  to  $\mathbb{R}^{1,2} \times S^1$ . In the future, when the ghosts are far away, one finds an asymptotically flat space in which a (non-singular) string-like object has formed. The ‘core’ of the string is an infinite throat where a spatial direction is compactified into a circle of shrinking radius. The geometry is time-dependent, and presumably contains Einstein-Rosen cylindrical gravitational waves produced in the nucleation event.

In order to compute the Euclidean action for the instanton we shall use the results in the previous section. The appearance of a new asymptotic region down the throat does not give any additional contribution to the action of (87): one can easily check that the Gibbons-Hawking boundary term  $\int \sqrt{\gamma} K$  vanishes at the boundary at  $x = +1$ . Hence we can directly read off the result from eq. (87), after making the parameter choices appropriate for this solution. We find

$$I_E = -\frac{\pi}{2GA}(c_0 - c_1) = -\frac{\pi m_-}{A} = -2\pi G m_-^2. \quad (100)$$

This action is *negative*. However, as we have explained in section 2 above, this does not imply an exponentially enhanced catastrophic decay. Rather, the production rate is always suppressed, and is

$$\Gamma \sim e^{-|I_E|} = e^{-2\pi G m_-^2}. \quad (101)$$



## 4.2 Conjuring up ghosts in deSitter space

In the previous subsection we have seen that the materialization of a pair of ghosts (without accompanying normal particles) results in the formation of a new asymptotic region in the shape of an infinite throat inbetween the ghosts, with a compactified spatial circle. The creation of such a new infinity may sound a little disturbing and may cast some doubt on the whole construction. We saw in sec. 2 that ghost domain wall formation in flat space also came associated with the appearance of a new asymptotic region. In that case, we found that the inclusion of a cosmological constant served to regularize the possible divergences of the infinite volume that arises after nucleation.

This suggests that we consider the decay of empty deSitter space via the materialization of two ghosts. Even if, as we will see, the appearance of an infinite throat is *not* avoided in this way, the issues of regularization of the Euclidean action are much simpler, since the Euclidean action of the instanton is already finite. The space left over as the ghosts fly apart is again deSitter, although, as was the case with the flat space at asymptotic future in the previous section, it has non-trivial global identifications.

The solution we seek is obtained from a generalization of the C-metric (91) to include a cosmological constant  $\Lambda = 3H^2$  [26]. Its metric can be written as

$$ds^2 = \frac{1}{A^2(x-y)^2} \left[ F(y)dt^2 + (1 + 2Gm_-A)^2 \left( -\frac{dy^2}{F(y)} + \frac{dx^2}{G(x)} \right) + G(x)d\phi^2 \right], \quad (102)$$

where

$$G(x) = (1 - x^2)(1 - 2Gm_-Ax), \quad F(y) = h^2 + (1 - y^2)(1 - 2Gm_-Ay), \quad (103)$$

and, to reduce clutter, we have defined

$$h = H \frac{1 + 2Gm_-A}{A}. \quad (104)$$

Again, we have already chosen the sign of the mass parameter (with  $m_- > 0$ ) to correspond to a ghost. It is obvious that as  $H \rightarrow 0$  we recover (91). The main difference with the latter is that the roots of  $G(x)$  and  $F(y)$  now do not coincide. As a consequence, while  $x$  still varies in the range  $[-1, 1]$ , now  $y \in [-\infty, y_0]$ , where  $y_0$  is the only real root that  $F(y)$  has when  $m_-A > 0$  and  $H^2 > 0$ . Since  $y_0 < -1$ , the asymptotics of space differ from (91):  $y = y_0$  is the deSitter horizon, and no spatial infinity can be reached (we will see that  $y \rightarrow x$  is future infinity). As before,  $y = -\infty$  is the naked singularity of the ghost.

The  $(x, \phi)$  sector in (102) is exactly the same as in (91), so the analysis of the geometry of (93) in the previous section applies again: we remove the conical singularity at  $x = -1$  by identifying  $\phi \sim \phi + 2\pi$ . To eliminate the singularity at  $x = 1$ , the only choice is eq. (90),

which pushes it down a throat an infinite spatial distance away. Hence the appearance of a new asymptotic region is not avoided. Looking down the throat using the coordinate  $\zeta$  of eq. (95), and inside the deSitter horizon, the geometry is well approximated by

$$ds^2 \simeq \frac{1}{A^2(1-y)^2} \left[ F(y) d\hat{t}^2 - 4 \frac{dy^2}{F(y)} + 2 (d\zeta^2 + e^{-2\zeta} d\phi^2) \right], \quad (105)$$

which is qualitatively similar to the case without a cosmological constant, eq. (97).

As before, we are also interested in investigating the asymptotic future evolution of the geometry. In this case we have to go beyond the future deSitter horizon, to the region where  $y_0 < y < x$ . There, the spacelike future infinity characteristic of deSitter appears by taking  $y \rightarrow x \in [-1, 1]$ , where  $x$  is now one of the coordinates parameterizing future infinity. Close to the pole at  $x = -1$  (*i.e.*, away from the throat) the future asymptotic geometry approaches deSitter space. To see this, consider  $1 + x \ll x - y \simeq 1 + y$ , and introduce new coordinates

$$1 + x = \frac{A^2 r^2}{4}, \quad \frac{2H}{A^2} \hat{t} = w, \quad 1 + y = e^{-H\tau}, \quad (106)$$

to recover exponentially expanding deSitter space

$$ds^2 \rightarrow -d\tau^2 + e^{2H\tau} (dw^2 + dr^2 + r^2 d\phi^2). \quad (107)$$

Near the opposite pole at  $x = +1$ , we are in the throat region. The future asymptotic metric is also locally equivalent to deSitter space, which can be made manifest by introducing, besides the coordinate  $\zeta$  in (95), new coordinates (compare to (98))

$$w = \frac{\sqrt{2}}{A} \hat{t}, \quad \sinh H\tau = \frac{\sqrt{2}H}{A(1-y)} \quad (108)$$

in terms of which

$$ds^2 \rightarrow -d\tau^2 + \frac{1}{H^2} \sinh^2(H\tau) (d\zeta^2 + e^{-2\zeta} d\phi^2) + \cosh^2(H\tau) dw^2. \quad (109)$$

If the coordinate  $\phi$  were non-compact and ranged over the entire real line, this would be equivalent to the portion of deSitter space that lies beyond the cosmological horizon (an “upper wedge” akin to the Milne region of Minkowski space). However, like in the previous section,  $\phi$  must be periodic by continuity of the full solution across the horizon. Hence, the asymptotic geometry in the region close to the axis that runs between the ghosts is deSitter space with a periodic spatial circle. Of course, as  $\tau \rightarrow \infty$  the exponential expansion inflates the size of this circle, at any finite value of  $\zeta$ , so eventually it becomes effectively non-compact.

The Euclidean instanton is obtained by Wick-rotating  $\hat{t} \rightarrow it_E$ . Regularity (up to the naked ghost singularity, which we assume is smoothed out by ghost matter) requires the identification

$$t_E \sim t_E + \frac{8\pi}{F'(y_0)}, \quad (110)$$

associated to the finite temperature of the deSitter horizon.

In order to compute the Euclidean action we use again (84), which allows us to avoid dealing with the specific action for ghost matter, as long as it satisfies the Einstein equations. There is no contribution from the boundary of the infinite throat since the Gibbons-Hawking term vanishes there. The acceleration horizons now are actually cosmological horizons, which are finite without the need for regularization. The reference background is deSitter space with the same value for  $H$ , and a simple calculation yields

$$I_E = \frac{\pi}{2GH^2}(1 + y_0). \quad (111)$$

Since  $1 + y_0 < 0$ , this action, like in the asymptotically flat case considered earlier, is always negative, but the decay rate is exponentially suppressed as  $\Gamma \sim e^{-|I_E|}$ .

To illustrate this result, we consider a small cosmological constant and expand in powers of  $H^2 G^2 m_-^2$  (*i.e.*, the square of the ratio between the gravitational size of the lump and the Hubble radius). We find

$$I_E \simeq -2\pi G m_-^2 (1 - 4H^2 G^2 m_-^2 + \dots). \quad (112)$$

In the limit  $H \rightarrow 0$  we correctly recover our previous result (100).

## 5 Discussion

We have studied theories with ghosts (“the Others”) that interact very weakly, through gravity, with the ordinary world. Empty space can decay into ghosts and ordinary particles, and we have focussed on the possibility that non-relativistic lumps of ghost matter be produced by tunneling processes, involving only curvature scales smaller than  $\mu$ .

In ordinary field theory, nucleation rates are usually estimated by using instanton methods, as  $\Gamma \sim e^{-I_E}$ , where  $I_E$  is the corresponding action. We have computed  $I_E$  for a variety of such possible decays. In some cases (eqs. (15), (100), (111)),  $I_E$  has turned out to be negative. Naively, this would appear to lead to an exponentially enhanced catastrophic decay rate. However, the Euclidean path integral (even in the absence of gravity) in theories with ghosts is ill-defined, and the standard Euclidean rules do not apply. In section 2 we have discussed nucleation processes using the canonical WKB approach, without reference to Euclidean methods. We have argued that for systems of a single degree of freedom,

and for tightly bound systems of ghost and ordinary matter, the nucleation rates should be estimated as

$$\Gamma \sim e^{-|I_E|}. \quad (113)$$

This formula may not be valid if, besides the gravitational interaction between ghosts and matter, there are other dominant forces contributing to the tunneling (such as the expansion of the universe). Here, we are mainly interested in the case when ghosts and matter nucleate from nearly flat space, and the tunneling is possible due to the gravitational energy-momentum transfer between matter and ghosts. In this situation, we expect (113) to be valid. In more general cases, we expect that Eq. (113) represents only a conservative upper bound to the nucleation rate. Investigation of this more general case is left for further research.

A first class of decays involves the nucleation in flat space of lumps of ordinary matter together with their ghost counterparts. For the spontaneous nucleation of diwalls (an asymptotically flat configuration of concentric walls, with an ordinary wall chasing after a ghost wall), the corresponding Euclidean action is given by Eq. (15). If the tensions of the two walls are very different in magnitude, the action is of the form  $|I_E| \sim M_P^6/\sigma_1^2$ , where  $\sigma_1$  is the tension of the ordinary wall. If both tensions are very similar, then the action is parametrically given by

$$|I_E| \sim \frac{M_P^6}{\sigma^2} \frac{\delta\sigma}{\sigma}. \quad (114)$$

The curvature radius of the walls is given by  $R \sim 1/G\sigma$ , so the above formula takes the form  $|I_E| \sim M_P^2 R \delta R$ . The effective theory (1) is supposed valid only at distance scales larger than the cutoff  $\mu^{-1}$ , so within the regime of validity of this effective theory,

$$|I_E| \gtrsim \left(\frac{M_P}{\mu}\right)^2 \simeq 10^{60} \quad (115)$$

so the process of diwall nucleation is extraordinarily suppressed,  $\Gamma \sim e^{-10^{60}}$ .

Such suppression does not appear to be at work in the nucleation of a pair of Bondi dipoles (the non-perturbative analogue of (3)), for which we have computed the action to be

$$I_E \simeq 2\pi m_+ d, \quad (116)$$

where  $m_+$  and  $d$  are the mass and size of the dipole. There is no obvious Planck-scale suppression here. However, since we require  $d \gtrsim \mu^{-1}$ , the process will be suppressed for all lumps whose mass  $m$  is much larger than  $\mu$ . In the context of the Standard Model with parity symmetry, the only elementary particles which might have a mass comparable to the gravitational cut-off scale are neutrinos. Could we then have non-perturbative nucleation of neutrinos and ghost-neutrinos? The existence of the corresponding instanton requires that the ordinary particle have larger mass than its ghost counterpart, eq. (81). Now, the

symmetry between the normal and ghost sectors is broken only by their different coupling to gravity. So any differences between the masses of a particle and its ghost must be due to self-energy corrections from the coupling to gravity. Since normal particles are gravitationally attractive, whereas ghosts are repulsive, the gravitationally-induced corrections to the mass will be

$$(\Delta m_+^2)_{\text{grav}} < 0, \quad (\Delta m_-^2)_{\text{grav}} > 0. \quad (117)$$

These work in a direction opposite to (81), and therefore the dangerous decay appears to be not simply suppressed but actually forbidden!

Lastly, we have analyzed the non-perturbative analogue of (6). This involves a dramatic topology change mediated by an instanton with negative Euclidean action

$$I_E \simeq -2\pi G m_-^2. \quad (118)$$

As we have seen, the negative sign does not spell doom since we should use (113) for the decay rate. If we demand that the size of the nucleated configuration  $\sim A^{-1} \sim G m_-$  be larger than the cutoff scale  $\mu^{-1}$ , then this process is as strongly suppressed as (115), and therefore imposes no phenomenological constraints.

The decays of flat space involving ghost matter that we have studied do not, by any means, exhaust all possibilities. We have considered ghost domain walls and ghost particles, but ghost cosmic strings can also unstabilize the vacuum. A ghost cosmic string coupled to gravity creates a conical excess. If the string is open with ghost monopoles at its endpoints (*i.e.*, the string is topologically unstable) then the string will pull the monopoles together: such strings can not pop out of the vacuum spontaneously. However, string vortices, even topologically stable ones, can end on black holes [27]. If a ghost string has black holes (which necessarily have positive mass) at its endpoints, then the string will push the black holes apart. One can then envisage a process in which one such ghost string with two black holes attached is nucleated out of the flat vacuum. Following [28], the relevant instanton can be easily constructed, and the action is

$$I_E \simeq \frac{\pi m^2}{T} - \pi G m^2 = \frac{\pi m^2}{T} \left( 1 - \frac{T}{M_P^2} \right), \quad (119)$$

where  $m$  is the mass of the black holes and  $T$  the absolute value of the ghost string tension. The first contribution in (119) is the nucleation rate of the string itself, and the second is an enhancement of the decay due to black hole entropy<sup>5</sup>. The latter becomes subleading for string tensions  $T \ll M_P^2$ , so the factor in brackets in (119) can be taken to be of order one.

---

<sup>5</sup>In order to construct the instanton the black holes must be charged and extremal (or almost extremal) [28], so their entropy is  $S_{bh} \simeq \pi G m^2$ .

In order that the size of the nucleated configuration be larger than the gravitational cutoff we must require  $m/T \gtrsim \mu^{-1}$ . Since the black holes must also be larger than Planck size,  $m \gtrsim M_P$ , we find that

$$I_E \gtrsim \frac{M_P}{\mu} \sim 10^{30}. \quad (120)$$

Again, the nucleation rate is strongly suppressed.

The results presented in this paper are quite encouraging for the energy-parity-symmetric theory in (1). In all the cases where we have found the possibility to conjure ghosts, we have seen they can be exorcized away for all of eternity (for practical purposes), in the sense that  $|I_E|$  is always extremely large for the non-perturbative decay processes considered. Nevertheless, it should be kept in mind that the Euclidean path integral is ill-defined in theories with a ghost sector, and our justification of Eq. (113) for the nucleation rates is rather heuristic. In this sense, our analysis should be regarded as preliminary. A more rigorous derivation of nucleation rates in theories with ghosts deserves further investigation. One might also worry that the suppression of the decay seems to be of a different sort in each of the cases we have studied: while (114), (118), (119) are suppressed by the weakness of gravity, the Bondi pair production (116) is instead eliminated by dynamical considerations. There does not seem to be an underlying generic argument that guarantees that ghost decays are always phenomenologically harmless. Here we have considered what appear to be the simplest and most natural decay channels, but we cannot rule out the existence of a different and dangerous non-perturbative instability.

## Acknowledgements

This work is partially supported by grants CICyT FPA2004-04582-C02-02, European Commission FP6 program MRTN-CT-2004-005104, and DURSI 2005SGR 00082.

## Appendix: Tunneling paths

In Section 2.4 we considered the nucleation of walls and diwalls using the canonical WKB approach. Although the explicit form of the tunneling path was not needed in order to integrate the Hamilton-Jacobi equation, it remains to be shown that such path can be constructed. Also, in order to remove a certain sign ambiguity [see the discussion around Eq. (47)] we assumed that there is a path where the momentum associated with the position of the wall vanishes,  $p = 0$ , or where  $V_+ = V_-$ . Here, we discuss the construction of such paths. Again, we follow the approach of Ref. [14] (with minor modifications to accommodate the case of compact geometries).

Eqs. (35) with  $p = 0$  can easily be solved for  $\hat{R}'_{\pm} \equiv R'(r = q \pm \epsilon)$ :

$$\frac{\hat{R}'_{\pm}}{L} = \frac{1}{2} \left( \frac{(V_- - V_+)}{4\pi G\sigma \hat{R}} \mp 4\pi G\sigma \hat{R} \right). \quad (121)$$

Likewise, from (34), we can find the momentum  $\hat{\Pi}_L \equiv \Pi_L(r = q)$ ,

$$\hat{\Pi}_L^2 = \frac{\hat{R}^2}{G^2} \left( \frac{(V_+ - V_-)^2}{64\pi^2 G^2 \sigma^2 \hat{R}^2} - \frac{V_+ + V_-}{2} + 4\pi^2 G^2 \sigma^2 \hat{R}^2 - 1 \right). \quad (122)$$

For instance, in the case when the cosmological constants are the same on both sides of the wall, we can take the turning point before tunneling to be regular inside the wall, so that  $M_- = 0$ , but allow for an infinitesimal mass of the initial bubble  $M_+ \neq 0$ . In this case  $V_- = 1 - H^2 \hat{R}^2$  and  $V_+ = 1 - H^2 \hat{R}^2 - 2GM_+/\hat{R}$ . The momentum is given by

$$\hat{\Pi}_L^2 = \frac{\hat{R}^2}{G^2} \left\{ H^2 \hat{R}^2 + \left( 2\pi G\sigma \hat{R} + \frac{M_+}{4\pi\sigma \hat{R}^2} \right)^2 - 1 \right\}.$$

The zeroes of the quantity in curly brackets define the turning points. In the limit when  $M_+ \rightarrow 0$ , one of the turning points tends to zero (vanishing initial size)

$$\hat{R}_b \approx (M_+/4\pi\sigma)^{1/2} \rightarrow 0,$$

and the other is given by the size of the wall at the moment of nucleation

$$\hat{R}_a = R_w = [H^2 + (2\pi G\sigma^2)]^{-1/2}.$$

In this limit, the expression simplifies to  $\hat{\Pi}_L^2 = G^{-2} \hat{R}^2 [1 - (H^2 + (2\pi G\sigma)^2) \hat{R}^2]$ .

Let us first consider the case of negative tension walls nucleating in deSitter. For given radius of the wall  $\hat{R}$ , we can find a three geometry by solving the following differential equations:

$$\left( \frac{R'}{L} \right)^2 = 1 + V(R) + \frac{G^2 \hat{\Pi}_L^2}{\hat{R}^2} \left( \frac{R}{\hat{R}} \right)^2, \quad (r < q), \quad (123)$$

$$\left( \frac{R'}{L} \right)^2 = (1 + V(R)) \left\{ 1 + \frac{G^2 \hat{\Pi}_L^2}{\hat{R}^2 (1 + V_+(\hat{R}))} \right\}. \quad (r > q). \quad (124)$$

These 3-geometries will automatically satisfy the appropriate junction conditions at  $R = \hat{R}$ . They will also correspond to the turning point geometries when  $\hat{\Pi}_L = 0$ , that is, when  $\hat{R} = \hat{R}_a$  or  $\hat{R} = \hat{R}_b$ . For intermediate values of  $\hat{R}$ , they interpolate between turning points. The sequence of 3-geometries is schematically represented in Fig. 4. It is important that for  $R \rightarrow 0$  we have  $R'/L \rightarrow 1$ , so that the geometry is locally flat at the origin, inside the

wall. On the other hand, right outside the wall, Eq. (121) shows that the radius is growing  $\hat{R}'_+ > 0$ , hence it is natural to choose a boundary condition such that as we approach the horizon  $1+V=0$ , we have  $R'=0_+$ . This geometry can either be continued analytically past the horizon, or simply matched smoothly with the original turning point solution beyond the horizon (leaving the part beyond the horizon unchanged throughout the whole semiclassical path.) For  $r < q$ , we have  $V = -H^2 R^2$ , and Eq. (123) leads to

$$R(y) = \alpha^{-1} \cos \alpha y, \quad (r < q), \quad (125)$$

where  $y$  stands for proper distance,  $dy = Ldr$ , and

$$\alpha^2 \equiv H^2 - \frac{G^2 \hat{\Pi}_L^2}{\hat{R}^4} > H^2. \quad (126)$$

In the last inequality, we have used that  $\hat{\Pi}_L^2 < 0$  under the barrier. Thus, the geometry inside of the wall is just that of a cap of a three-sphere of radius  $\alpha^{-1}$ . At the first turning point, when  $\hat{R} = \hat{R}_b \approx (M_+/4\pi\sigma)^{1/2}$ ,  $\hat{\Pi}_L$  vanishes and the curvature radius is “large”,  $\alpha^{-1} = H^{-1}$ . However, as  $\hat{R}$  grows to be a few times  $\hat{R}_a$ , we find that the second term in (126) quickly dominates, and the curvature radius of the three sphere becomes much smaller,  $\alpha^{-1} \sim (M_+/\sigma)^{1/2}$  (vanishingly small as  $M_+$  tends to zero). The curvature radius of the geometry inside the bubble grows back to its original size  $\alpha^{-1} = H^{-1}$  as the second turning point is approached. The solution outside the bubble is obtained by integrating Eq. (124). Note that the term in curly brackets in the right hand side is just a constant, and so the solution is basically the warp factor of an “Anti”-Schwarzschild-deSitter geometry (with negative mass parameter  $M_+ < 0$ ), with “Hubble” parameter  $H$ , but with an unconventional parametrization. For instance, in the limit  $M_+ \rightarrow 0$  we have

$$R(y) \approx H^{-1} \cos \beta H y, \quad (r > q),$$

where  $\beta < 1$  is the square root of the term in curly brackets in Eq. (124). The 3-geometry always contains a maximal circle of the size of the horizon of the (fictitious) “Anti”-Schwarzschild-deSitter geometry. In particular, the 3-volume is large for any value of  $\hat{R}$ . In the limit  $M_+ \rightarrow 0$  (and ignoring the fact that a small part of the volume is cut out by the bubble) the 3-volume scales like  $V_3 \sim 1/\beta H^3$ . Hence, we have found a sequence of three geometries interpolating between both turning points, where the 3-volume is always of the order  $H^{-3}$  or larger. This is in contrast with the picture where the three geometry first disappears and then reappears with a large bubble in it.

For walls of positive tension, we can construct interpolating geometries along the same lines. However, for Eq. (121) now shows that in the limit  $M_+ \rightarrow 0$  and finite  $\hat{R}$ , the radius  $R(r)$  is always decreasing right outside the bubble  $\hat{R}'_+ < 0$ . Hence, it is convenient to



choose the boundary condition for  $r > q$  in a form appropriate to decreasing radii. Thus, instead of (124) we can use (123) also outside the bubble. The sequence of 3-geometries is schematically represented in Fig. 3. Initially, in the limit of small mass  $GM_+ \ll H^{-1}$ , the geometry is basically that of a 3-sphere of radius  $H^{-1}$  with a small spherical wall of radius  $\hat{R} = \hat{R}_b \sim (M_+/\sigma)^{1/2}$ . As we increase  $\hat{R}$  to a few times  $\hat{R}_b$ , the curvature radius of the geometry on both sides of the wall becomes comparable to the radius of the wall. As  $\hat{R}$  is further increased, the geometry on both sides becomes more and more symmetric, corresponding to two spherical caps of curvature radius  $\alpha^{-1}$ . As we approach the second turning point,  $\hat{R} = \hat{R}_b = R_w$ , this curvature radius becomes  $H^{-1}$ . In this case, the path we are considering first shrinks the spatial geometry to a very small size  $\sim (M_+/\sigma)^{1/2}$ , and then the new geometry grows from this seed. Thus, in the present case, if we take the limit when  $M_+ \rightarrow 0$ , the initial geometry disappears and the new one reappears from “nothing”.

Finally, we may consider the paths for nucleation of diwalls. In this case, the construction of a path with  $p = 0$  seems rather tricky, because there are two independent wall radii. Instead, since the instanton in this case has the trivial topology of  $R_4$ , we can construct a semiclassical path by simply slicing the instanton on surfaces of constant coordinate  $T \equiv y \cos \chi$ , where  $\chi$  is the polar coordinate on the three-spheres. For  $T \rightarrow -\infty$  the geometry is that of flat three-dimensional Euclidean space, while for  $T = 0$  we have the turning point with two nested domain walls. The potential vanishes everywhere,  $V = 0$ , and hence the equality  $V_+ = V_-$  is trivially satisfied across each wall. This justifies the use of Eq. (47) in this case too.

## References

- [1] D. E. Kaplan and R. Sundrum, “A symmetry for the cosmological constant,” arXiv:hep-th/0505265.
- [2] A. D. Linde, “The Inflationary Universe,” Rept. Prog. Phys. **47** (1984) 925.
- [3] R. R. Caldwell, “A Phantom Menace?,” Phys. Lett. B **545** (2002) 23 [arXiv:astro-ph/9908168].
- [4] S. M. Carroll, M. Hoffman and M. Trodden, “Can the dark energy equation-of-state parameter  $w$  be less than -1?,” Phys. Rev. D **68** (2003) 023509 [arXiv:astro-ph/0301273].
- [5] J. M. Cline, S. Jeon and G. D. Moore, “The phantom menaced: Constraints on low-energy effective ghosts,” Phys. Rev. D **70** (2004) 043543 [arXiv:hep-ph/0311312].

- [6] A. Anisimov, E. Babichev and A. Vikman, “B-inflation,” JCAP **0506** (2005) 006 [arXiv:astro-ph/0504560].
- [7] H. Bondi, “Negative Mass in General Relativity,” Rev. Mod. Phys. **29**, 423 (1957).
- [8] W. Israel and K. A. Khan, “Collinear particles and Bondi dipoles in General Relativity,” Nuovo. Cim. **33**, 331 (1964).
- [9] W. B. Bonnor and N. S. Swaminarayan, “An exact stationary solution of Einstein’s equations,” Z. Phys. **186**, 222 (1965).
- [10] G. W. Gibbons, “The motion of black holes,” Commun. Math. Phys. **35** (1974) 13.
- [11] A. Vilenkin, “Gravitational field of vacuum domain walls,” Phys. Lett. B **133** (1983) 177.
- [12] W. Israel, “Singular hypersurfaces and thin shells in General Relativity,” Nuovo Cim. B **44S10** (1966) 1 [Erratum-ibid. B **48** (1967 NUCIA,B44,1.1966) 463].
- [13] R. Basu, A. H. Guth and A. Vilenkin, “Quantum creation of topological defects during inflation,” Phys. Rev. D **44**, 340 (1991).
- [14] W. Fischler, D. Morgan and J. Polchinski, “Quantization Of False Vacuum Bubbles: A Hamiltonian Treatment Of Gravitational Tunneling,” Phys. Rev. D **42** (1990) 4042.
- [15] G. T. Horowitz and R. C. Myers, “The value of singularities,” Gen. Rel. Grav. **27**, 915 (1995) [arXiv:gr-qc/9503062].
- [16] J. L. Synge, “Relativity: The General Theory” (North Holland, Amsterdam, 1960).
- [17] H. F. Dowker and S. N. Thambyahpillai, “Many accelerating black holes,” Class. Quant. Grav. **20** (2003) 127 [arXiv:gr-qc/0105044].
- [18] R. Emparan and H. S. Reall, “Generalized Weyl solutions,” Phys. Rev. D **65** (2002) 084025 [arXiv:hep-th/0110258].
- [19] W. Kinnersley and M. Walker, “Uniformly Accelerating Charged Mass In General Relativity,” Phys. Rev. D **2**, 1359 (1970).
- [20] W. B. Bonnor, “The sources of the vacuumC-metric,” Gen. Rel. Grav. **15**, 535 (1983).
- [21] G. Gamow, “Biography of Physics” (Harper & Row, New York, 1961).

- [22] R. Emparan, “Massless black hole pairs in string theory,” *Phys. Lett. B* **387** (1996) 721 [arXiv:hep-th/9607102]; “Composite black holes in external fields,” *Nucl. Phys. B* **490** (1997) 365 [arXiv:hep-th/9610170].
- [23] S. W. Hawking and G. T. Horowitz, “The Gravitational Hamiltonian, action, entropy and surface terms,” *Class. Quant. Grav.* **13**, 1487 (1996) [arXiv:gr-qc/9501014].
- [24] K. Hong and E. Teo, “A new form of the C-metric,” *Class. Quant. Grav.* **20**, 3269 (2003) [arXiv:gr-qc/0305089].
- [25] R. Emparan and M. Gutperle, “From p-branes to fluxbranes and back,” *JHEP* **0112**, 023 (2001) [arXiv:hep-th/0111177].
- [26] J. F. Plebanski and M. Demianski, “Rotating, Charged, And Uniformly Accelerating Mass In General Relativity,” *Annals Phys.* **98**, 98 (1976).
- [27] A. Achúcarro, R. Gregory and K. Kuijken, “Abelian Higgs hair for black holes,” *Phys. Rev. D* **52** (1995) 5729 [arXiv:gr-qc/9505039].
- [28] S. W. Hawking and S. F. Ross, “Pair production of black holes on cosmic strings,” *Phys. Rev. Lett.* **75**, 3382 (1995) [arXiv:gr-qc/9506020].  
R. Emparan, “Pair creation of black holes joined by cosmic strings,” *Phys. Rev. Lett.* **75**, 3386 (1995) [arXiv:gr-qc/9506025].  
D. M. Eardley, G. T. Horowitz, D. A. Kastor and J. H. Traschen, “Breaking cosmic strings without monopoles,” *Phys. Rev. Lett.* **75**, 3390 (1995) [arXiv:gr-qc/9506041].